

001  
002  
003  
004  
005  
006  
007  
008  
009  
010  
011  
012  
013  
014  
015  
016  
017  
018  
019  
020  
021  
022  
023  
024  
025  
026  
027  
028  
029  
030  
031  
032  
033  
034  
035  
036  
037  
038  
039  
040  
041  
042  
043  
044  
045  
046

# Microbial symbionts buffer hosts from the demographic costs of environmental stochasticity

Joshua C. Fowler<sup>1,2\*</sup>, Shaun Ziegler<sup>3</sup>, Kenneth D. Whitney<sup>3</sup>,  
Jennifer A. Rudgers<sup>3</sup>, Tom E.X. Miller<sup>1</sup>

<sup>1</sup>\*Department of BioSciences, Rice University, Houston, 77005, TX, USA.

<sup>2</sup>Department of Biology, University of Miami, Miami, 33146, FL, USA.

<sup>3</sup>Department of Biology, University of New Mexico, Albuquerque, 87131, NM, USA.

\*Corresponding author(s). E-mail(s): [jcf221@miami.edu](mailto:jcf221@miami.edu);

Contributing authors: [shaun.ziegler@gmail.com](mailto:shaun.ziegler@gmail.com); [whitneyk@unm.edu](mailto:whitneyk@unm.edu);

[jrudgers@unm.edu](mailto:jrudgers@unm.edu); [tom.miller@rice.edu](mailto:tom.miller@rice.edu);

Phone: 719-359-2960

#### Author Contributions

J.C.F. contributed to data collection, data analysis, and led manuscript drafting. S.Z. contributed to data collection and manuscript revisions. K.D.W. contributed to research conception, data collection, and manuscript revisions. J.A.R. established transplant plots, contributed to research conception, data collection, and manuscript revisions. T.E.X.M. contributed to research conception, data collection, data analysis, and manuscript revisions.

#### Data and Code Accessibility

Data will be made accessible as an Environmental Data Initiative package online  
**DOI:** [updated here when available](#). Code for all analysis is available through  
<https://github.com/joshuacfowler/Grass-Endophyte-Stochastic-Demography>

**Article Type:** Letter

**Running Title:** Symbiont-mediated demographic buffering

**Keywords:** stochastic demography, plant-microbe interactions, environmental variability, symbiosis, mutualism, long-term data, life history, Epichloë, Poaceae

**This file contains:** Abstract ( 150 words), Main Text (5000 words), Figures (1-5); Supporting Information - Supplemental Methods, Supplemental Figures S1-S89, Supplemental Tables S1-S3, References (84)

047  
048  
049  
050  
051  
052  
053  
054  
055  
056  
057  
058  
059  
060  
061  
062  
063  
064  
065  
066  
067  
068  
069  
070  
071  
072  
073  
074  
075  
076  
077  
078  
079  
080  
081  
082  
083  
084  
085  
086  
087  
088  
089  
090  
091  
092

### Abstract

Species' persistence in increasingly variable climates will depend on resilience against the fitness costs of environmental stochasticity. Most organisms host microbiota that shield against stressors. Here, we test the hypothesis that, by limiting exposure to temporally variable stressors, microbial symbionts reduce hosts' demographic variance. We parameterized stochastic population models using data from a 14-year symbiont-removal experiment including seven grass species that host *Epichloë* fungal endophytes. Results provide novel evidence that symbiotic benefits arise not only through improved mean fitness, but also through damped inter-annual variance. Hosts with "fast" life history traits benefited most from symbiont-mediated demographic buffering. Under current climate conditions, contributions of demographic buffering were modest compared to benefits to mean fitness. However, simulations of increased stochasticity amplified benefits of demographic buffering and made it the more important pathway of host-symbiont mutualism. Microbial-mediated variance buffering is likely an important, yet cryptic, mechanism of resilience in an increasingly variable world.

Introduction	093
Global climate change involves <del>increases</del> heterogenous changes in environmental variability, including <del>changes to precipitation patterns and increases in</del> the frequency of extreme weather events [? ?] and of “whiplash events” that alternate between climate extremes [? ? ? ?]. Yet, the ecological consequences of <del>increased</del> changing variability are less well understood than those of changing <del>climate</del> means, such as long-term warming or drying. Incorporating environmental variability into forecasts of population dynamics can improve <del>predictions of the future</del> future predictions [?].	094 095 096 097 098 099 100 101 102 103 104 105 106 107 108 109 110 111 112 113 114 115 116 117 118 119 120 121 122 123 124 125 126 127 128 129 130 131 132 133 134 135 136 137 138
Classic theory predicts that long-term population growth rates (equivalently, population mean fitness) will decline under increased environmental stochasticity because <del>the</del> costs of bad years outweigh <del>the</del> benefits of good years – a consequence of nonlinear averaging [? ? ]. For example, in unstructured populations, the long-term stochastic growth rate in a fluctuating environment ( $\lambda_s$ ) will always be lower than the <del>average growth rate</del> <del>(<math>\bar{\lambda}_t</math>)</del> arithmetic mean of annual growth rates ( $\bar{\lambda}_t$ ) by an amount proportional to the environmental variance ( $\sigma^2$ ):	$\log(\lambda_s) \approx \log(\bar{\lambda}_t) - \frac{\sigma^2}{2\bar{\lambda}_t^2} \quad (1)$
Populations structured by size or stage <del>similarly experience costs of experience similar costs of temporal</del> variability [? ? ]. There are accordingly two pathways to increase population viability in <del>a variable environment</del> variable environments: increase the arithmetic mean growth rate and/or dampen temporal fluctuation in growth rates, also called “ <del>variancee</del> -demographic buffering”.	
Both <del>the inherent</del> characteristics of species and the <del>properties of their environment environments they experience</del> can buffer demographic fluctuations, <del>including</del> . Inherent characteristics include life history traits <del>such as longevity</del> [? ? ], <del>correlations</del> [? ] , trade-offs among vital rates [? ], and transient shifts in population structure [? ]. For example, theory predicts long-lived species, those on the slow end of the <del>magnitude of environmental variability</del> [? ], or the <del>degree of environmental</del> slow-fast life history continuum, to be less sensitive to environmental variability than short-lived species [? ], a pattern with empirical support across plants [? ? ] and animals [? ? ]. Demographic variance is also determined by external abiotic factors, such as the magnitude of environmental variability [? ] or environmental autocorrelation [? ? ]. <del>These factors determine the risks of extinction faced by populations</del> [? ] <del>and underlie</del> The complex interplay of these factors determines populations’ risk of extinction [? ] and <del>underlies</del> management strategies promoting ecosystem resilience [? ]. Yet, little is known about how <del>biotic interactions influence demographic variability or contribute to variancee</del> inter-specific interactions influence contribute to demographic buffering [? ].	
Most multicellular organisms host symbiotic microbes that affect growth and performance [? ? ], <del>and many of these</del> many of which are vertically transmitted from maternal hosts to offspring [? ]. Vertical transmission links the fitness of hosts and symbionts in a feedback loop that selects for mutual benefits [? ]. <del>Many vertically transmitted microbes are mutualistic and</del> These mutualistic microbes can protect hosts from stressful	

139 environmental conditions including drought, extreme temperatures, or natural ene-  
140 mies [? ? ]. Some ~~of the best~~<sup>well</sup> studied examples include bacterial symbionts of  
141 insects that provide ~~their~~ hosts with thermal tolerance through the production of heat-  
142 shock proteins [? ], and fungal symbionts of plants that produce anti-herbivore and  
143 drought-protective compounds [? ? ? ]. However, these diverse protective symbioses  
144 are context-dependent: the magnitude of benefits depends on environmental condi-  
145 tions [? ]-[? ? ] and thus will vary temporally in ~~a stochastic environment~~ stochastic  
146 environments [? ]. We hypothesized that context-dependent benefits from symbionts  
147 may buffer ~~hosts~~ host populations against variability through strong benefits during  
148 harsh periods and neutral or even costly outcomes during benign periods, reducing  
149 the impacts of host exposure to extremes and dampening inter-annual variance rela-  
150 tive to non-symbiotic hosts -(Fig. 1A). Variance buffering is a previously unexplored  
151 mechanism by which symbionts may benefit their hosts instead of or in addition to  
152 elevating average fitness (Fig. 1C), the focus of most previous research.

153 ~~We~~-To test the hypothesis that context-dependent benefits of symbiosis dampen  
154 interannual variance in host fitness, we used a combination of long-term field experi-  
155 ments and stochastic demographic modeling~~to test the hypothesis that context-dependent~~  
156 ~~benefits of symbiosis buffer hosts from the fitness costs of environmental stochasticity~~. We  
157 used cool-season grasses and *Epichloë* fungal endophytes~~as~~, a tractable experimental  
158 model in which non-symbiotic plants can be derived from naturally symbiotic plants  
159 through heat treatment, providing a contrast of symbiont effects that controls for the  
160 confounding influence of host genetic background. *Epichloë* endophytes are special-  
161 ized symbionts growing intercellularly in the aboveground tissue of ~ 30% of *C<sub>3</sub>* grass  
162 species [? ]. These fungi are primarily transmitted vertically from maternal plants  
163 through seeds [? ]. They produce a variety of alkaloids that can protect host plants  
164 from natural enemies [? ] and drought stress [? ].

165 Over 14 years (2007–2021), we collected longitudinal demographic data on the  
166 survival, growth, reproduction, and recruitment of all plants within replicated  
167 endophyte-symbiotic and endophyte-free populations at our field site in southern Indi-  
168 ana, USA. Through taxonomic replication (seven host-symbiont species pairs) we  
169 aimed to understand whether host life history traits could explain inter-specific vari-  
170 ation in the magnitude of demographic buffering through symbiosis. We used this  
171 long-term data to parameterize Bayesian stochastic population projection models~~in-a~~  
172 ~~hierarchical Bayesian framework~~. Specifically, we (1) quantified the effect of symbiosis  
173 on the mean and variance of host vital rates (survival, growth and reproduction) and  
174 fitness, (2) evaluated the relationship between host life history traits and the magni-  
175 tude of symbiont-mediated variance buffering, (3) determined the relative ~~contribution~~  
176 ~~contributions~~ of symbiont-mediated mean and variance effects to host fitness, and  
177 (4) projected how increased environmental stochasticity (expected under future cli-  
178 mates) changes the importance of variance buffering as a pathway of host-symbiont  
179 mutualism.

180

181

182

183

184

<b>Materials and Methods</b>	185
<b>Study site and species</b>	186
This study was conducted at Indiana University's Lilly-Dickey Woods Research and Teaching Preserve (39.238533, -86.218150) in Brown County, Indiana, USA. This site is part of the Eastern broadleaf forests of southern Indiana, where the ranges of many understory cool-season grass species overlap. <b>The experiment</b> We focused on seven of these grasses ( <i>Agrostis perennans</i> , <i>Elymus villosus</i> , <i>Elymus virginicus</i> , <i>Festuca subverticillata</i> , <i>Lolium arundinaceum</i> , <i>Poa alsodes</i> , and <i>Poa sylvestris</i> ), each of which hosts a unique species of <i>Epichloë</i> endophyte (Table S1). All are native to eastern North America except the Eurasian species <i>L. arundinaceum</i> .	187
<b>Endophyte removal, plant propagation, and field set-up</b>	188
<del>Seeds from Seeds from local, naturally symbiotic populations of the seven focal host species were collected during summer-fall 2006 from Lilly-Dickey Woods and the nearby Bayles Road Teaching and Research Preserve (39.220167, -86.542683). To generate symbiotic (S+) and symbiont-free (S-) plants from the same genetic lineages, seeds from each species 2006. Seeds were disinfected with a heat treatment described in Table S1 or left untreated. The heat treatment created to generate symbiont-free plants by warming seeds to temperatures at which the fungus becomes inviable but the host seeds can still germinate. Both heat-treated and untreated seeds were surface sterilized with bleach to remove epiphyllous microbes, cold stratified for up to 4 weeks, then germinated in a growth chamber before transfer to the greenhouse at Indiana University where they grew for ~8 weeks. We confirmed endophyte status by staining thin sections of inner leaf sheath with aniline blue and examining tissue for fungal hyphae at 200X magnification [? ]. We established experimental populations with vegetatively propagated clones of similar sizes. By starting the experiment with plants of similar sizes and the same number of unique genotypes, we aimed to limit any potential effects of heat treatments on initial plant growth [? ].</del>	189
<del>During the (S-) and symbiotic (S+) plants from the same genetic lineages. In fall of 2007 and spring of 2008, we established 10 3x3 m plots for <i>A. perennans</i>, <i>E. villosus</i>, <i>E. virginicus</i>, <i>F. subverticillata</i>, and <i>L. arundinaceum</i> and 18 plots for <i>P. alsodes</i> and <i>P. sylvestris</i>. Half of the plots were Each plot was randomly assigned to be planted with either 20 evenly spaced symbiotic (S+) or symbiont-free (S-) plants, and initiated with 20 evenly spaced individuals labeled with aluminum tags. In spring 2008, we placed plastic deer net fencing around each plot to limit deer herbivory and disturbance; damaged fences were regularly replaced. Full details of endophyte removal, plant propagation and field set-up are provided in Supporting Information - Supplemental Methods and Table S1.</del>	190
<b>Long-term demographic data collection</b>	191
Each summer (2008–2021) we censused all individuals in each plot for survival, growth and reproduction, and added new recruits to the census. Plots contained 13.3 individuals/m <sup>2</sup> on average over the course of the experiment during the study. Each census year was a sample of inter-annual climatic variation (n = 14 years, comprising 13 demographic transition years). We censused each species during its peak fruiting stage	192
	193
	194
	195
	196
	197
	198
	199
	200
	201
	202
	203
	204
	205
	206
	207
	208
	209
	210
	211
	212
	213
	214
	215
	216
	217
	218
	219
	220
	221
	222
	223
	224
	225
	226
	227
	228
	229
	230

231 (May: *Poa alsodes*, *Poa sylvestris*; June: *Festuca subverticillata*; July: *Elymus villosus*,  
232 *Elymus virginicus*, *Lolium arundinaceum*; September: *Agrostis perennans*), such that  
233 the censuses were pre-breeding and new recruits came from the previous years' seed  
234 production –(Fig. S1 shows a generalized life cycle diagram). Leaf litter was cleared  
235 out of each plot prior to before the census, to aid in locating plants. For each plant  
236 remaining from the previous year tagged plant, we determined survival, measured its size  
237 as a count of tillers, and collected reproductive data as counts of reproductive tillers  
238 and seed-bearing spikelets on all reproductive tillers up to three up to three  
239 reproductive tillers. We also tagged all unmarked individuals that were recruits from  
240 the previous years' seed production and collected the same demographic data. New  
241 recruits typically had one tiller and were non-reproductive. In 2008 through 2010,  
242 we took additional counts of seeds per inflorescence for all reproducing individuals in  
243 the plots to relate inflorescence and spikelet counts to seed production. In 2018, we  
244 stopped collecting data for the exotic *L. arundinaceum*, which had very high survival  
245 and low recruitment, and consequently very low variation in population  
246 size across years. In total across 14 years, the dataset included demographic information  
247 for 16,789 individual host-plants and 31,216 transition-year observations.

248 We expected plots to maintain their endophyte status (symbiotic or symbiont free)  
249 because these fungal symbionts are almost exclusively vertically transmitted, and plots  
250 were spaced a minimum of 5 m apart, limiting seed dispersal or horizontal transmission  
251 of the symbiont between plots. However, we regularly confirmed endophyte treatment  
252 throughout the lifetime of the experiment by opportunistically taking subsets of seeds from  
253 reproductive individuals and scoring them for their endophyte status with microscopy as  
254 above. Overall, these scores reflected 98% faithfulness of recruits to their expected endophyte  
255 status across species and plots (Fig. S23; Supplement data). Additionally, we have rarely  
256 observed fungal stromata, the fruiting bodies by which *Epichloë* are potentially transmitted  
257 horizontally, provided the fly vector is also present [?]. For *A. perennans*, *F. subverticillata*,  
258 *L. arundinaceum*, and *P. alsodes*, we never observed stromata. We observed stromata only  
infrequently for *E. villosus*, and even more rarely for *E. virginicus* and *P. sylvestris* (Table  
259 S2). For these species, stromata have only been observed irregularly across years on 35, 4,  
and 6 plants respectively, making up < 0.3% of all censused plants.

## 259 Vital rate modeling

260 Equipped with these demographic data, we fit statistical models for survival, growth,  
261 flowering (yes or no) adult survival, seedling survival, adult growth, seedling growth, repro-  
262 ductive status (flowering or vegetative), fertility of flowering plants (number of flowering  
263 tillers inflorescences), production of seed-bearing spikelets (number per inflorescence), the  
264 average number of seeds per spikelet, and the recruitment of seedlings from the preceding  
265 year's seed production. We fit these vital rates as generalized linear mixed models in a hierar-  
266 chical Bayesian framework using RStan [?] which allowed us to isolate endophyte effects on  
267 vital rate means and variances, borrow strength across species for some variance components,  
268 and propagate uncertainty from the individual-level vital rates to population projection mod-  
269 els [?]. All vital rate models included random plot and year effects, with separate estimates  
270 of year-to-year variance for symbiotic and symbiont-free plants, to quantify size-structured  
271 models included the same linear predictor, including two key parameters for each species:  
272 one which described the effect of endophytes on inter-annual variance. All parameters were  
273 given vague priors [?]. We ran each vital rate model for 2500 warm-up endophyte symbio-  
274 sis on the mean of that vital rate, and 2500 MCMC sampling iterations with three chains.  
275 We assessed model convergence with trace plots of posterior chains and checked for  $\hat{R}$  values  
276 less than 1.01, indicating low within- and between-chain variation [? ?]. For those models  
that showed poor convergence, we extended the MCMC sampling to include 5000 warm-up  
and 5000 sampling iterations, which was only necessary for seedling growth. We graphically  
checked vital rate model fit with posterior predictive checks comparing simulated and observed  
277 data (Fig. S19-S20).

<i>Survival</i> — We modeled survival as a Bernoulli process, where the survival ( $S$ ) of an individual $i$ in plot $p$ and census year $t$ was predicted by the plot-level endophyte status ( $e$ ), host species ( $h$ ), size in the preceding census, and the plant's origin status (whether it was initially transplanted or naturally recruited into the plot).—	277
	278
	279
Here, $\hat{S}$ is the survival probability, $\beta_{0,h}$ is an intercept another which described inter-annual variance in the vital rate for symbiotic and symbiont-free plants, estimated using random year effects specific to each host species , $\beta_1$ is the effect of the plant's recruitment origin, $\beta_{2,h}$ is the endophyte effect, $\beta_{3,h}$ is the size effect, $\tau_{e,h,t}$ is a normally distributed year effect for each species species and endophyte statuswith variance $\sigma_{\tau_{e,h}}^2$ , and $\rho_p$ is a normally distributed plot effect with variance $\sigma_p^2$ ( $p(e)$ indicates that plot identity is uniquely associated with an endophyte status). We assume that origin effect $\beta_1$ and plot-to-plot variance $\sigma_p^2$ are shared across host species, allowing us to “borrow strength” across the multi-species dataset; other model parameters are unique to host species. We separately modeled the survival of newly recruited seedlings with a similar model but omitting previous size dependence and origin status.—	280
	281
	282
	283
	284
	285
	286
	287
	288
	289
	290
	291
	292
	293
	294
	295
	296
	297
	298
	299
	300
	301
	302
	303
	304
	305
	306
	307
	308
	309
	310
	311
	312
	313
	314
	315
	316
	317
	318
	319
	320
	321
	322
<i>Growth</i> — We modeled plant size in census year $t$ ( $G$ ) with the same linear predictor for the mean as described for survival. Because we measured size as positive integer valued counts of tillers, we modeled it with a zero-truncated Poisson-inverse Gaussian distribution. This distribution includes a shape parameter $\lambda_G$ to account for overdispersion in the data. We additionally modeled the growth of newly recruited seedlings separately with a Poisson-inverse Gaussian model omitting size structure and the plants' origin status as with seedling survival.—	290
	291
	292
	293
	294
	295
	296
	297
	298
	299
	300
	301
	302
	303
	304
	305
	306
	307
	308
	309
	310
	311
	312
	313
	314
	315
	316
	317
	318
	319
	320
	321
	322
<i>Flowering</i> — We modeled whether or not a plant was flowering during the census ( $P$ ) as a Bernoulli process, with the same linear predictor for the mean as described above for survival except that size dependence for reproductive vital rates was determined by the individual's size during the same census year as opposed to its size during the previous year.—	290
	291
	292
	293
	294
	295
	296
	297
	298
	299
	300
	301
	302
	303
	304
	305
	306
	307
	308
	309
	310
	311
	312
	313
	314
	315
	316
	317
	318
	319
	320
	321
	322
<i>Fertility</i> — For a plant that was flowering during the census, its fertility was the number of reproductive tillersproduced ( $F$ ), which we modeled as a function of size in the same census period with a zero-truncated Poisson-Inverse Gaussian distribution, with the same linear predictor for the mean as described above.—	290
	291
	292
	293
	294
	295
	296
	297
	298
	299
	300
	301
	302
	303
	304
	305
	306
	307
	308
	309
	310
	311
	312
	313
	314
	315
	316
	317
	318
	319
	320
	321
	322
<i>Spikelets per Inflorescence</i> — Spikelet production ( $K$ ) was recorded as integer counts on up to three inflorescences per reproducing plant. We modeled these data with a negative binomial distribution, with the same linear predictor for the mean as described above.—	290
	291
	292
	293
	294
	295
	296
	297
	298
	299
	300
	301
	302
	303
	304
	305
	306
	307
	308
	309
	310
	311
	312
	313
	314
	315
	316
	317
	318
	319
	320
	321
	322
<i>Seed Production per Spikelet</i> — For individuals with recorded counts of seed production, we calculated the number of seeds per spikelet from our counts of seeds and spikelets per inflorescence, and then modeled seeds per spikelet ( $D$ ) as means of a Gaussian distribution for each species and endophyte status. Because we had less detailed data across years and plants for seed production than for other reproductive vital rates, we omitted both plot and year random effects.—	290
	291
	292
	293
	294
	295
	296
	297
	298
	299
	300
	301
	302
	303
	304
	305
	306
	307
	308
	309
	310
	311
	312
	313
	314
	315
	316
	317
	318
	319
	320
	321
	322
<i>Seedling Recruitment</i> — We used a binomial distribution to model the recruitment of new seedlings ( $R$ ). This species- and endophyte status- specific random year effect allowed us to quantify effects of endophytes on inter-annual variance for each vital rate. Other parameters accounted for size structure in the data (defined as the number of tillers) as well as differences between originally transplanted plants (started in a greenhouse) and those which recruited naturally into the plotsfrom seeds produced in the preceding year, assuming no long-lived seed bank. We included an intercept specific to each host and endophyte status and the same random effects structure as in other models. We estimated the number of seeds per plot in the preceding year by multiplying the total number of reproductive tillers per plant by the mean number of spikelets per inflorescence and mean number of seeds per spikelet ( $D$ ). For plants with missing fertility or spikelet data, we used the expected number of reproductive tillers ( $F$ ) or of spikelets per inflorescence from ( $K$ ), drawing from the full posteriors of our models.—	290
	291
	292
	293
	294
	295
	296
	297
	298
	299
	300
	301
	302
	303
	304
	305
	306
	307
	308
	309
	310
	311
	312
	313
	314
	315
	316
	317
	318
	319
	320
	321
	322

323 **Stochastic population model**

324 ~~Using the fitted~~

325

## 326 Stochastic population model

327 We built stochastic matrix projection model for each host species. We parameterized the mod-  
328 els using the fitted statistical vital rate models, we parameterized stochastic matrix projection  
329 models including in a manner similar to continuous IPM models [?], while accounting for  
330 the discrete data representing our focal species' growth [?]. Each matrix projection model  
331 included two state variables:  $r_t$  (the number of newly recruited individuals in year  $t$  which  
332 we assume to be non-reproductive), and  $\mathbf{n}_t$  (a vector including all non-seedling individuals  
333 of discrete sizes  $x \in \{1, 2, \dots, U\}$ , ranging from one to the maximum number of tillers  $U$ ). We  
334 use these two state variables to avoid having to assume assuming demographic equivalence  
335 between seedling and non-seedling one-tiller plants. We used the same model structure, cor-  
336 responding to a pre-breeding census, for each species and endophyte status (not shown in  
337 model notation, to make it more readable for readability; Fig. S1).

336 The number of recruits in year  $t + 1$  is given by:

337

$$338 r_{t+1} = \sum_{x=1}^U P(x; \boldsymbol{\tau}_P) F(x; \boldsymbol{\tau}_F) K(x; \boldsymbol{\tau}_K) D R(\boldsymbol{\tau}_R) n_t^x \quad (2)$$

339

340 The total number of seeds produced by a maternal plant of size  $x$  is the product of the  
341 size-specific probability of flowering  $P$ , the number of reproductive tillers inflorescences con-  
342 ditional on flowering  $F$ , the number of spikelets per inflorescence  $K$ , and the number of  
343 seeds per spikelet  $D$ . Multiplying by the probability of transitioning from seed to seedling  $R$   
344 gives a per-capita rate of seedling production, which is multiplied by the number of plants  
345 of size  $x$  ( $n_t^x$ , the  $x^{\text{th}}$  element of  $\mathbf{n}_t$ ) and summed over all sizes. Each function also depends  
346 on the species- and endophyte-specific year random effects for that vital rate ( $\boldsymbol{\tau}$ , a vector of  
347 year-specific values derived from the statistical models).

346 The number of  $y$ -sized plants in year  $t + 1$  is given by:

347

$$348 n_{t+1}^y = Z(y; \boldsymbol{\tau}_Z) B(\boldsymbol{\tau}_B) r_t + \sum_{x=1}^U S(x; \boldsymbol{\tau}_S) G(x, y; \boldsymbol{\tau}_G) n_t^x \quad (3)$$

349

350

351 where  $n_{t+1}^y$  is the  $y^{\text{th}}$  element of vector  $\mathbf{n}_{t+1}$ . The first term on the right hand side of Eqn.  
352 ?? represents growth ( $Z$ ) and survival ( $B$ ) of seedling recruits. The second term includes the  
353 survival of previously  $x$ -sized plants and the growth of survivors from size  $x$  to  $y$ , summed  
354 over all  $x$ . To avoid predictions of unrealistic growth outside of the observed size distribution,  
355 we set a ceiling on capped the growth function for plants at the 97.5<sup>th</sup> percentile of observed  
356 sizes for each host species [?]. We analyzed projection models constructed from parameters  
357 representing the dynamics of naturally recruited plants.

358 Each of the vital rate functions vital rate function in Eqns. ?? and ?? have has separate  
359 intercepts and year random effects for symbiotic and symbiont-free populations, allowing  
360 us to calculate the effect of endophyte symbiosis on the mean, variance, and coefficient of  
361 variation (CV) of  $\lambda_t$ , the dominant eigenvalue of the year- and endophyte-specific projection  
362 matrix. This model treats climate drivers implicitly through year-specific random effects. We  
363 also developed a climate-explicit version with the addition of additional parameters defining  
364 the relationship between either annual or growing season drought index and each vital rate  
365 (*Supporting Information - Supplemental Methods*).

366 To calculate stochastic population growth rates ( $\lambda_S$ ) for each host species and endophyte  
367 status we simulated population dynamics for 1000 years by randomly sampling from the  
368 13 annual transition matrices, discarding the first 100 years to minimize the influence of  
369 initial conditions. Sampling observed transition matrices (rather than independently sampling  
370 regression coefficients) produces models that realistically capture inter-annual variation by  
371 preserving vital rate correlations [?]. We tallied total population size at each time step as  
372  $N_t = r_t + \sum_{x=1}^U n_t^x$  and calculated the stochastic growth rate as  $\log(\lambda_S) = E[\log(\frac{N_t}{N_{t+1}})]$

[? ? ]. We calculated total effects of endophyte symbiosis as the difference in  $\lambda_S$  between S+ and S- populations. We propagated uncertainty from the vital rates to the calculation of  $\lambda_S$  using 500 draws from model posteriors.

A full description of climate-explicit methods can be found in the *Supporting Information - Supplemental Methods*.

## Life History Analysis

We collected metrics describing each host species' life history to test the relationship between pace of life and variance buffering (Table S1). Using the Rage package [? ], we calculated  $R_0$ , longevity, and generation time from our estimated transition matrices using the symbiont-free mean matrix as the reference condition. We recorded seed size as the average lemma length from the Flora of North America [? ]. We also calculated the 99th percentile of maximum observed age for each species from their S- symbiont-free plants from the census data for each species. Using the Rage package [? ], we calculated generation time, longevity, net reproductive rate  $R_0$ , Keyfitz entropy (describing survivorship across lifespan), and Demetrius entropy (describing reproduction across lifespan) from the mean transition matrix for symbiont-free populations. Next, we fit Bayesian phylogenetic mixed-effects models using the brms package [? ] to test the relationship between each life history trait and the effect of symbiosis on the CV of  $\lambda_t$  (a measure of variance buffering) while controlling for phylogenetic non-independence between host and symbiont species. We pruned species-level phylogenies of plants [? ] and *Epichloë* fungi [? ] to include the focal species *Agrostis perennans* was not included in the tree, and so we used the congener *A. hyemalis*. We (or a congener for one host), and defined separate phylogenetic covariance matrices for each pruned tree. We propagated from these pruned trees for host and symbiont species. We propagated uncertainty in the estimated variance buffering effect  $V$  with a measurement error model.

Here,  $V_{EST}$  is the variance buffering effect for host species  $h$ , estimated from the posterior mean ( $V_{MEAN}$ ) and standard deviation ( $V_{SD}$ ), propagating uncertainty associated with the effect of symbiosis. The model includes an intercept ( $\alpha$ ) and a slope ( $\beta$ ) defining the relationship between the variance buffering effect and the life history trait. The residual standard deviation is given by ( $\sigma$ ). We used weakly informative priors to aid model convergence. Each prior was centered at zero, except for the residual standard deviation, which we centered at the standard deviation of the estimated variance buffering effect, .04. The phylogenetic random effect ( $\pi$ ), which is modeled as a multivariate normal distribution, has a between-species standard deviation ( $\sigma_\pi$ ) structured by the phylogenetic covariance matrix  $A$ . We ran each MCMC sampling chain for 8000 warmup iterations and 2000 sampling iterations. We assessed model convergence as described for the vital rate models. The statistical analysis is described in full in the *Supporting Information - Supplemental Methods*.

## Mean-variance decomposition

To calculate stochastic population growth rates ( $\lambda_s$ ) for each host species and endophyte status we simulated population dynamics for 1000 years by randomly sampling from the 13 annual transition matrices, discarding the first 100 years to minimize the influence of initial conditions. Sampling observed transition matrices produces models that realistically capture inter-annual variation by preserving correlations between vital rates [? ]. We tallied the total population size at each time step as  $N_t = r_t + \sum_{x=1}^U n_t^x$  and calculated the stochastic growth rate as  $\log(\lambda_s) = E[\log(\frac{N_t}{N_{t+1}})]$  [? ? ]. We calculated the total effect of endophyte symbiosis as the difference in  $\lambda_s$  between S+ and S- populations. We propagated uncertainty from the vital rate models to the calculation of  $\lambda_s$  using 500 draws from the posterior distribution of model parameters.

We decomposed the total endophyte effect on  $\lambda_s$ . We decomposed total endophyte effects on  $\lambda_S$  into contributions from effects on vital rate means, variances, and their interaction and variances. Specifically, we repeated the calculation of  $\lambda_S$  S+ and S-  $\lambda_S$  described above for two additional "treatments": (1) endophyte effects on mean vital rates only, with inter-annual variances shared between S+ and S- at the S- reference level for all vital rates, and (2) endophyte effects on vital rate variances only, with vital rate means shared between S+ and S- at the S- reference level. The combination of all four  $\lambda_S$ - $\lambda_S$  treatments (S+ vital rate means and variances, S- means and variances, S+ means with S- variances, S- means with

415 S+ variances) allowed us to quantify to what extent the overall effect of symbiosis derives the  
416 extent that overall effects of symbiosis derive from changes in vital rates means, variances, and  
417 their interaction. The interaction occurs because the variance penalty to stochastic growth is  
418 proportional to the mean value-arithmetic mean of annual growth rates (see as in Eq. 1, for  
419 example) such that variance is more detrimental for populations with lower average growth  
420 rates.

421 To create To quantify how mean and variance effects of symbionts arise through effects  
422 on different vital rates, we performed an additional decomposition described in *Supporting*  
*Information Supplemental Methods* that isolates symbiont effects on growth and survival from  
423 effects on fertility and recruitment.

424 We simulated scenarios of increased variance relative to that observed during the study period, we repeated the stochastic growth rate decomposition, but sampling only a subset  
425 our study by sampling subsets of the 13 observed annual transition matrices. We created two  
426 scenarios of increased environmental variance by sampling the transition matrices associated  
427 with the set of either six or two most extreme  $\lambda_t$  values, representing the six or two  $\lambda_t$  values  
428 for S- populations. These extreme  $\lambda_t$  values represent the best and worst years, using S-  
429 populations as the reference condition, experience by symbiont-free populations. By sampling  
430 away from an average year in both directions, the six- and two- years scenarios increased  
431 the standard deviation of yearly annual host growth rates by 1.3 and 2.1 times, respectively,  
432 without changing mean growth rates (<2.3 < 2.1% difference in  $\bar{\lambda}$  between simulation  
433 treatments, Fig. S21S79). We performed the same mean-variance decomposition for these  
434 scenarios as for the ambient conditions (all 13 years sampled) for all host species described  
435 above.

## 436 ResultSand Discussion

### 437 Symbionts buffer host demographic variance

438 Across seven host species, eight vital rates,

439 Across 14 years, and 16,789 individual plants, our analysis provided the first empirical  
440 evidence of symbiont-mediated variance buffering. Endophytes census years, endophytes  
441 reduced inter-annual variance for 66% (37/56) of host species-vital rate combinations (average  
442 Cohen's D for effects on vital rate standard deviation: -0.15) (Fig. 4A, 2A; Fig. S6-S22  
443 - Fig. S18S29). Endophytes also increased mean vital rates for the majority (36/56) of host  
444 species-vital rate combinations (average Cohen's D for effects on vital rate mean: 0.15), and  
445 benefits were particularly strong for host survival, plant growth and recruitment (Fig. 4A2A;  
446 Fig. S1-S2 - Fig. S5S11). The magnitude of mean and variance effects differed among host  
447 species-hosts and vital rates. Symbiont effects on vital rate variance were as large and even  
448 exceeded mean effects for certain species. For example, endophytes modestly increased mean  
449 adult survival (Fig. 4C) and 2C) and strongly reduced variance in survival (Fig. 4D2D) for  
450 *Festuca subverticillata*, while for *Poa alsodes*, variance buffering was more apparent in seedling  
451 growth and inflorescence production (Fig. 4E). Interestingly, certain 2E). Additionally, some  
452 vital rates showed costs of endophyte-symbiosis. Symbiotic individuals of *A. perennans* grew  
453 larger than those without endophytes symbiont-free hosts (Fig. 4B2B), yet endophytes also  
454 reduced this species' mean recruitment rates (Fig. 1A). In addition, endophyte symbiosis  
455 increased variance in 2A). Similarly, endophytes increased variance for certain species' vital  
456 rates, including seedling growth for *Elymus villosus* and *Festuca subverticillata* (Fig. 4A2A).

457 Because not all vital rates contribute equally to fitness, we used stochastic matrix models  
458 to integrate the diverse effects on vital rates diverse vital rate effects described above into  
459 comprehensive measures for the arithmetic mean and variance of year-to-year fitness ( $\lambda_t$ ) and  
460 the long-run stochastic fitness that integrates both mean and variance ( $\lambda_S$ ). On average  
461 across host species, mean fitness of S+ populations had greater mean fitness increased by  
462 more than 10% (> 92% confidence that endophytes increased  $\bar{\lambda}$ ) and lower  $\bar{\lambda}_t$ ) and inter-  
463 annual variability in fitness was 26% lower (> 86% confidence that endophytes decreased the  
464 coefficient of variation of  $\lambda_t$ ) than S- populations (Fig. 23). For some host species, the CV  
465 of  $\lambda_t$  declined by as much as 170 more than 62% (*P. alsodes*, *F. subverticillata*), while for  
466 others, endophyte effects on variance were substantially smaller (65% lower for *E. villosus*,  
467 1613% lower for *A. perennans*), or even positive (2737% increase for *E. virginicus*). When  
468 Considering mean and variance effects of symbionts were considered together, none of the

host-symbiont pairings were antagonistic (i.e., with endophytes that both decreased mean fitness and increased variance) (Fig. 2C)	461
, suggesting that variation across host species and vital rates in mean and variance effects may reflect alternative strategies that yield similar net benefits of endophyte symbiosis.	462
3C)	463
Reduced sensitivity to drought, as has been reported for some <i>Epichloë</i> symbioses [?]	464
, is a candidate mechanism that could generate a signature of variance buffering: drought conditions may have weaker fitness costs for S+ hosts, reducing fluctuations in fitness through time. Accordingly, analysis of climate-explicit matrix models indicated that, for five of seven taxa, S+ populations were less sensitive to annual or growing season drought (12-month or 3-month drought index; Standardized Precipitation-Evapotranspiration Index [?]) than S- populations (Supporting Information Text; Fig. S24-S25; Table S3). However, we did not find a strong relationship between the magnitude of variance buffering and relative drought sensitivities, suggesting that other climatic factors or other temporally varying aspects of the environment may elicit benefits of endophyte symbiosis, including documented resistance to herbivory for six of these host taxa [? ?].	465
	466
	467
	468
	469
	470
	471
	472
	473
<b>Faster life histories predict stronger symbiont-mediated variance buffering</b>	474
	475
	476
Theory predicts that long-lived species, those on the slow end of the slow-fast life history continuum, will be less sensitive to environmental variability than short-lived species [?]	477
, a pattern which has empirical support across plants [?] and animals [? ?]. Therefore, host species with long lifespans that produce few, large offspring should benefit less from symbiont-mediated variance buffering than species with fast life cycles that produce many smaller offspring with low per capita chance of success [? ?]. In support of this prediction, hosts with trait values representing faster life history strategies experienced greater Hosts with slow life history trait values experienced weaker variance buffering from endophytes than those with slow-fast life histories (Fig. 3). Bayesian phylogenetic mixed-effects models, controlling for species' relatedness, indicated that variancee 4). Variance buffering was stronger for host species with shorter lifespan (Fig. 3A; 754A; 67% probability of positive relationship with empirically observed maximum plant age) and smaller seeds (Fig. 3B; 734B; 65% probability of positive relationship with seed length). Other life history traits similarly had positive, but weaker, weak, positive support for the prediction that faster life history traits correlate with stronger variance buffering (Fig. S26-S28). Considering fungal life history traits, the three host species for which the net mutualism benefit was weakest ( <i>Elymus villosus</i> , <i>Elymus virginicus</i> , and <i>Poa sylvestris</i> ) (Fig. 2C) were the only hosts for which we observed fungal stromata, fruiting bodies capable of horizontal (contagious) transmission S83-S85). Models indicate moderate phylogenetic signal in the effect of variance buffering (average Pagel's $\lambda$ of 0.22 (90% CI: 0-0.8) and of 0.56 (90% CI: 0-0.9) from models including host and symbiont phylogeny respectively (Table S2). This result supports the theoretical expectation that strict vertical transmission drives the evolution of strong host-symbiont mutualism [? ?]. Conclusions about life histories are somewhat constrained by the narrow range of trait values among closely related species in the grass sub-family Pooideae and their co-evolving symbionts. Our understanding of how life history variation modulates the fitness consequences of microbial symbiosis would profit from tests across a wider span of taxonomic groups [? ].	478
	479
	480
	481
	482
	483
	484
	485
	486
	487
	488
	489
	490
	491
	492
	493
	494
	495
	496
	497
<b>Contributions from variance buffering are weak relative to mean effects</b>	498
	499
	500
To evaluate the relative importance of mean fitness benefits and variance buffering as alternative pathways of mutualism, we decomposed the overall effect of the symbiosis on the stochastic growth rate stochastic growth rates $\lambda_S$ using simulations from the population models in four configurations. These included including either the full symbiosis effect (both mean and variance buffering effects), mean effects alone, variance effects alone, or neither mean nor variance effects. Overall, the full effect of symbiosis on $\lambda_S$ , averaged across host species, provided strong evidence of grass-endophyte mutualism (99% certainty of a positive total effect on $\lambda_S$ ) (Fig. 45; see Fig. S22-S81 for individual host species). Contributions	501
	502
	503
	504
	505
	506

507 to this full effect derived from both mean and variance buffering effects, as well as a slightly  
508 negative interaction (i.e., the combined influence of mean and variance effects was smaller  
509 than the sum of their individual effects). Endophytes' contributions to  $\lambda_S$  from mean effects  
510 were four times greater, averaged across species, than contributions from variance buffering  
511 (Fig. 45), suggesting that, under the regime of environmental variability represented by our  
512 14-year study, dampened fluctuations in fitness via variance buffering was a far-less important  
513 element of the benefits of symbiosis—symbiont benefits than increased mean fitness. Decom-  
514 posing this result further into contributions through different vital rates demonstrated that  
515 demographic buffering arose primarily from symbionts' effects on host survival and growth,  
516 rather than from effects on reproduction (Fig. S82). Results for individual host species were  
517 largely consistent with the-cross-species trends (FigS22, S71). The full effect of symbiosis on  
518  $\lambda_S$  was positive for seven out of eight five out of seven host species, with statistical confi-  
519 dence ranging from 66%–78% to > 99% certainty. The one exception was the host species  
520 exceptions were the hosts *P. sylvestris* and *A. perennans*, for which our analysis indicated  
521 that fungal endophytes were effectively neutral—effectively neutral symbionts in their overall  
522 fitness effect (45% and 55% and 57% posterior probability of positive and negative effects  
523 ; Fig-S22effects respectively; Fig. S71).

## 521 **Variance buffering strengthens under increased environmental 522 variability**

523 Simulations of increased environmental variability, a key prediction of climate change  
524 forecasts [?], indicated that mutualism with microbial symbionts, and their variance-buffering  
525 effects in particular, will take on increased importance for hosts in a more variable future  
526 climate. To simulate increased variability, we repeated the decomposition of  $\lambda_S$  for two alter-  
527 native forecast scenarios, randomly sampling transition matrices that represented either the  
528 six most extreme years experienced by each species or the or two most extreme years, sub-  
529 sets of the thirteen transition matrices across the 14-year study period. Increased variability  
530 elicited stronger mutualistic benefits of endophyte symbiosis (Fig. 3) than ambient variability  
531 (Fig. 5; overall effect of the symbiosis increased by > 130%~ 2fold). This increase was driven  
532 by increased contributions from the variance buffering mechanism—variance buffering (from a  
533 24%–16% contribution in the ambient scenario to a 66%–54% contribution in the most variable  
534 scenario) rather than from greater mean effects. In the most variable scenario, the relative  
535 importance of mean and variance effects reversed, with variance buffering contributions that  
536 were 1.5–1.2 times greater than contributions from mean benefitsmean contributions, averaged  
537 across species (Fig. 4).—

538 Thus, variance buffering – a cryptic microbial influence that manifests only over long  
539 time scales – is poised to become the dominant way in which grasses benefit from symbiosis  
540 with fungal endophytes in more variable climates of the future.  
541

## 542 **Conclusion**

543 Ecologists increasingly recognize the importance of symbiotic microbes for host organisms  
544 and the populations, communities, and ecosystems in which their hosts reside [? ? ? ?].  
545 Despite awareness of these ubiquitous interactions, long-term studies of microbial symbioses  
546 are very rare. Our analysis of

## 547 **Discussion**

548 Across seven host species, eight vital rates, 14 years, and 16,789 individuals, our analysis pro-  
549 vided the first empirical evidence, to our knowledge, of demographic buffering conferred by  
550 microbial symbionts. Our taxonomically-replicated, long-term field experiments that manip-  
551 ulated the presence/absence of fungal symbionts in plants demonstrates for the first time  
552 revealed that heritable microbes can commonly benefit hosts not only through improved mean  
553 fitness – the focus of most previous research – but also through buffering against environmen-  
554 tal variance. Our results provide an important advance to improve forecasts of the responses  
555 of populations (and symbionts) to increasing environmental stochasticity under global change,

suggesting that Benefits to mean fitness dominated the overall fitness advantage of endophyte	553
symbiosis under observed environmental variability, but simulation experiments point to a	554
dominant role for demographic buffering under increased temporal environmental stochasticity.	555
There is growing interest in demographic buffering as a potential source of resilience	556
against the increased stochasticity under global change [? ]. Our results suggest that biotic	557
interactions, and microbial mutualisms in particular, may be an under-appreciated mechanism	558
of demographic buffering. In fact, any interaction that is subject to context-dependence –	559
where the magnitude of cost or benefit depends on harshness of the environment –	560
holds potential to modify demographic variance across years (Fig. 1). However, long-term	561
experimental data required to detect such an influence are rarely available.	562
Taxonomic replication of host-symbiont pairs enabled us to generalize beyond the focal	563
taxa and facilitated inference about the <i>types</i> of species in which demographic buffering may	564
be more or less likely. Because host taxa with “slow” life history traits, such as long lifespan,	565
may be intrinsically buffered from environmental variability [? ? ? ], we predicted that	566
buffering effects of endophyte symbiosis would be stronger in hosts with faster pace of life.	567
Supporting this prediction, we found that shorter-lived and smaller-seeded host species expe-	568
rienced stronger reductions in demographic variance through endophyte symbiosis. Thus, <b>for</b>	569
<b>some host species</b> , microbial symbiosis may compensate for the lack of intrinsic tolerance of	570
variability conferred by “slow” slow life history traits. We found that, relative-to-mean fitness	571
Future studies may consider fungal life history traits, such as diversity in biologically-active	572
alkaloids, or the production of stromata - fruiting bodies capable of horizontal (contagious)	573
transmission. The host species for which the net mutualism benefit was greatest ( <i>F. subverti-</i>	574
<i>cillata</i> and <i>L. arundinaceum</i> ) (Fig. S81) were among those never observed to produce fungal	575
stromata (Table S2), potentially supporting theoretical expectations that strict vertical trans-	576
mission drives evolution of strong host-symbiont mutualism [? ? ]. We caution that inferences	577
on trait correlates of demographic buffering were subject to large uncertainties (Fig. S85-	578
S86), reflecting the relatively narrow taxonomic breadth that we considered (closely related	579
grass species in the sub-family Pooideae and their co-evolving symbionts). Understanding of	580
how life history variation modulates the fitness consequences of microbial symbiosis would	581
profit from tests across a wider span of plant and animal groups [? ]. We also found relatively	582
consistent, positive effects of endophyte symbiosis on stochastic fitness (Fig. S80), suggesting	583
that variation across host species and vital rates in mean and variance effects (Fig. 3C) may	584
reflect alternative strategies that yield similar net benefits.	585
While our results highlight symbiont-mediated demographic buffering as a potential	586
source of resilience against increased environmental stochasticity, much work remains to	587
connect symbiont effects on mean and variance to quantitative forecasts of host-symbiont	588
dynamics under global change. Like most temporally stochastic population projection models,	589
our approach quantified demographic variance across years (and simulated increasing	590
variance) without attributing its cause(s). Realistic forecasts for host-symbiont dynamics	591
under environmental change will require explicit connections between driver variables and	592
demographic responses. Reduced sensitivity to drought, as is common in <i>Epichloë</i> symbioses	593
[? ? ? ? ], is a candidate mechanism that could generate a signature of variance buffering:	594
drought conditions may less costly for S+ hosts, dampening the effects of drought years and	595
reducing fluctuations in fitness through time (Fig. 1). Preliminary climate-explicit analyses	596
indicated that symbionts reduced sensitivity to drought indices for five of seven host taxa	597
(Supporting Information Text; Fig. S88-S89; Table S3). However, we did not find a strong	598
relationship between magnitude of variance buffering and relative drought sensitivities, sug-	
gesting that other climatic factors or temporally-varying aspects of the environment may	
elicit benefits of symbiosis, including documented resistance to herbivory for six of these host	
taxa [? ? ]. Identifying the type and timescale of relevant drivers would allow more direct	
connections between demographic models and outputs from global climate models.	
Symbiont-mediated demographic buffering is a potential target of selection for improved	
holobiont fitness [? ] and carries implications for the evolution of bet-hedging strategies in	
variable environments. Demographic buffering may be considered a bet-hedging strategy if	
reduced temporal variance comes at the cost of arithmetic mean fitness [? ]. This may be	
unlikely in this system, where most host species exhibited both reduced variance and elevated	
mean fitness through symbiosis (Fig. 3C). However, the context-dependent fitness effects that	
underlie demographic buffering may favor other forms of evolutionary bet-hedging. Theory	
suggests that imperfect transmission (the production of S- offspring from S+ parent) may	
be an adaptive host strategy in spatially or temporally varying environments when fitness	
effects of symbionts are environment-dependent by extending phenotypic variance of offspring	

599 and improving the odds of some having the optimal symbiont status for their environment  
600 [? ? ? ]. Imperfect vertical transmission is well-documented in grass-endophyte symbioses [? ],  
601 including our focal taxa (Table S2), and could be incorporated into our model by dynamically  
602 linking S+ and S- populations [? ? ]. A further step could incorporate diverse symbiont  
603 partners (e.g. different strains of *Epichloë* fungi or multiple species within the microbiome)  
604 to understand how microbial diversity contributes to host genotypic and phenotypic variance  
[? ].

604 Several limiting features of our study point to new directions and valuable next steps. We  
605 focused explicitly on temporal variation and intentionally averaged over spatial heterogeneity.  
606 Endophytes may dampen spatial heterogeneity in host fitness in ways that parallel their effects  
607 on temporal variance, and this hypothesis could be explored by leveraging the plot replication  
608 in our experiment. At larger spatial scales, buffering effects of symbionts may vary across the  
609 broad geographic distributions of these eastern North American grass species, especially since  
610 historical and projected trends in climate variability are geographically heterogeneous [? ].  
611 Finally, our demographic modeling framework could be further “unpacked” to explore other  
612 elements of fitness in stochastic environments. We identified damping variance in survival  
613 and growth as the key avenue by which symbionts’ variance effects contributed to host fitness  
614 (Fig. S82). Elasticity analyses could explore the selection that drives diverse symbiont effects  
615 across host vital rates. Small changes in variance of vital rates that are highly important to  
616 population growth (i.e. those with high elasticities) may be more strongly selected for than  
617 larger changes in less important vital rates [? ], and symbionts may even provide an adaptive  
618 advantage by increasing temporal variance in certain vital rates (i.e. demographic lability)  
619 [? ]. Further, our simulations assumed that an independently distributed environmental state,  
620 but environmental auto-correlation can be an important component of stochastic population  
621 projections [? ] and might modify the fitness consequences of symbiont-mediated variance  
622 buffering. Similarly, correlated responses of multiple vital rates could amplify or dampen  
623 demographic variance [? ? ? ]. Our “matrix sampling” approach accounted for vital rate  
624 correlations implicitly [? ] but exploring whether and how endophyte symbiosis alters the  
625 correlation structure of host vital rates could add nuance to understanding of symbionts’  
626 contributions to variance buffering.

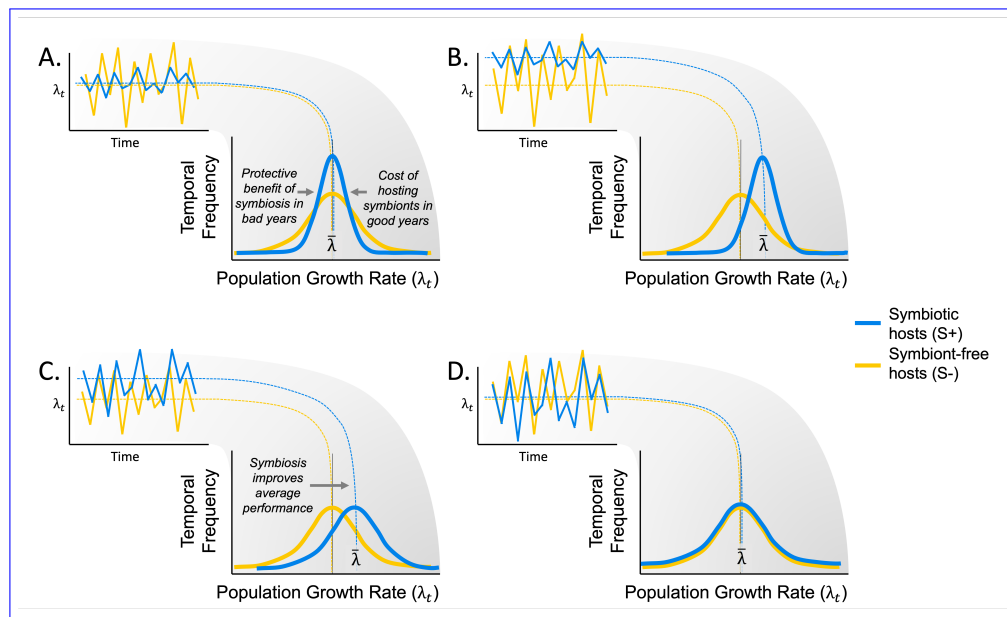
## 622 **Conclusion**

624 Ecologists increasingly recognize the importance of symbiotic microbes for host organisms  
625 and the populations, communities, and ecosystems in which their hosts reside [? ? ? ? ].  
626 Despite awareness of these ubiquitous interactions, long-term studies of microbial symbiosis  
627 are rare. Our results provide an important advance to improve forecasts of the responses of  
628 populations (and symbiota) to increasing environmental stochasticity under global change.  
629 We found that, relative to mean fitness benefits, symbiont-mediated variance buffering made  
630 weak contributions to host-symbiont mutualism under the current regime of observed environ-  
631 mental variability. However, demographic buffering is likely to become the dominant  
632 benefit that fungal endophytes confer to grass hosts in more variable future environments.  
633 Thus, demographic buffering – a cryptic microbial influence that manifests only over long  
634 time scales – is poised to become the dominant benefit of symbiosis. This result emerges from  
635 the context-dependent nature of grass-endophyte interactions, combined with the observation  
636 that environmental stochasticity generates fluctuation in context. These key ingredients, and  
637 thus the potential for symbiont-mediated variance buffering, similarly apply to the diverse  
638 host-microbe symbioses across the tree of life.

639  
640  
641  
642  
643  
644

<b>Acknowledgments.</b> We thank Mark Sheehan, Ali Campbell, Kyle Dickens, Blaise Willis, and Sar Lindner for contributions to field data collection. We also thank Volker Rudolf, Daniel Kowal, Lydia Beaudrot and Judie Bronstein for helpful comments on and discussion of this project. This research was supported by the National Science Foundation (grants 1754468 and 2208857).	645
<b>Supplementary information.</b> Supplementary information for this paper includes Supplementary Methods, Figs. A1 to A28, and Tables A1 to A3.	646
	647
	648
	649
	650
	651
	652
	653
	654
	655
	656
	657
	658
	659
	660
	661
	662
	663
	664
	665
	666
	667
	668
	669
	670
	671
	672
	673
	674
	675
	676
	677
	678
	679
	680
	681
	682
	683
	684
	685
	686
	687
	688
	689
	690

691 **Figures**  
 692  
 693  
 694



714 **Fig. 1 Endophyte** Hypothesized effects of symbiosis ~~altered host vital~~ on the mean and variance of  
 715 annual population growth rates. (A) ~~Shading represents the posterior mean standardized effect~~  
 716 size (Cohen's D) of endophyte Context-dependent symbiosis ~~on mean~~ may provide benefits to hosts  
 717 during harsh years while being neutral or ~~standard deviation~~ costly during benign years. Temporal  
 718 variance in populations growth rates of symbiotic host vital rates populations (S+; blue indicates  
 719 that symbiosis increased the mean or standard deviation and red indicates a reduction lines) is  
 720 expected to decrease relative to symbiont-free hosts (S-; yellow lines). Endophytes' diverse vital rate  
 721 effects include increased-(B) mean growth of *A. perennans* and Symbiosis may improve average  
 722 performance across years in addition to reducing temporal variance. (C) ~~mean survival probability~~  
 723 Consistent benefits of *F. subverticillata*. Endophyte presence also reduced inter-annual symbiosis  
 724 could improve average performance across years with no influence on temporal variance in-. (D) ~~the~~  
 725 survival of *F. subverticillata* and (E) the fertility of *P. alsodes* Symbiosis may have an effectively  
 726 neutral effect on population growth rates. In panels B-C, mean vital rate estimates are shown  
 727 with 80% credibles along with data binned by size for symbiotic (S+) and symbiont-free (S-)  
 728 plants, while in panels D-E, annual vital rate estimates are shown along with data binned by  
 729 size and census year. Organism silhouettes modified from "Festuca subverticillata" by Cindy  
 730 Roché and "Agrostis hyemalis" and "Poa alsodes" by Sandy Long ©Utah State University.  
 731  
 732  
 733  
 734  
 735  
 736

737  
738  
739  
740  
741  
742  
743  
744  
745  
746  
747  
748  
749  
750  
751  
752  
753  
754  
755  
756  
757  
758  
759  
760  
761  
762  
763  
764  
765  
766  
767  
768  
769  
770  
771  
772  
773  
774  
775  
776  
777  
778  
779  
780  
781  
782

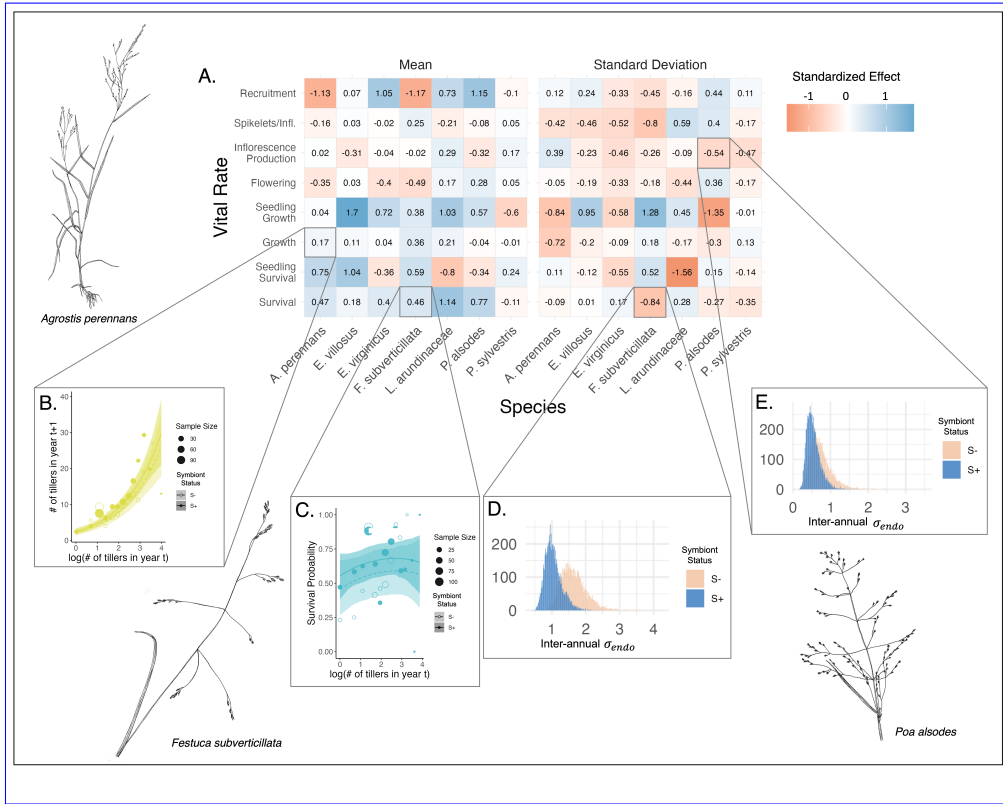


**Fig. 2** Endophyte symbiosis altered host vital rates.(A) Shading represents the posterior mean standardized effect size (Cohen's D) of endophyte symbiosis on mean or standard deviation of host vital rates (blue indicates that symbiosis increased the mean or standard deviation and red indicates a reduction). Endophytes' diverse vital rate effects include increased (B) mean growth of *A. perennans* and (C) mean survival probability of *F. subverticillata*. Endophyte presence also reduced inter-annual standard deviation in (D) the survival of *F. subverticillata* and (E) the fertility of *Poa alsodes*. In panels B-C, expected mean vital rates that average across years and plots are shown with 80% credible intervals along with points representing data binned by size for symbiotic (S+) and symbiont-free (S-) plants. Panels D-E show estimated posterior distributions of endophyte-status specific inter-annual standard deviation ( $\sigma_{r_{e,h}}^2$ ) for each vital rate for S+ (blue) and S- (beige) populations. Organism silhouettes modified from "Festuca subverticillata" by Cindy Roché and "Agrostis hyemalis" and "Poa alsodes" by Sandy Long ©Utah State University.

783

784

785

786

787

788

789

790

791

792

793

794

795

796

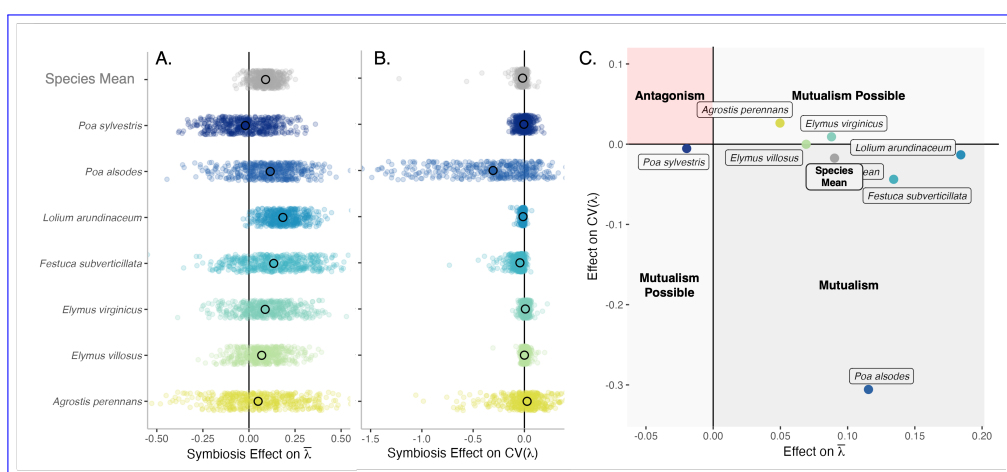
797

798

799

800

**Fig. 3** Mean and variance-buffering effects on fitness. Black circles indicate the average-posterior median effect of endophytes along with 500 posterior draws (smaller colored circles) on the (A) mean and (B) coefficient of variation in  $\lambda_t$  for each host species as well as a cross species mean. (C) For all hosts, endophytes either reduce variance, increase the mean, or both, and consequently when considering stochastic environments, the interactions are always at least potentially mutualistic.



801

802

803

804

805

806

807

808

809

810

811

812

813

814

815

816

817

818

819

820

821

822

**Fig. 4** Host species with faster life history traits experience stronger effects of symbiont-mediated variance buffering. Regressions between life history traits describing the fast-slow life history continuum ((A) 99th percentile maximum age observed during long term censuses in years; (B) Seed size) and the effect of endophyte symbiosis on the coefficient of variation in annual population growth rate ( $\text{CV}(\lambda_t)$ ). Each panel shows the fitted mean relationship (line) along with the 95% credible interval.

823

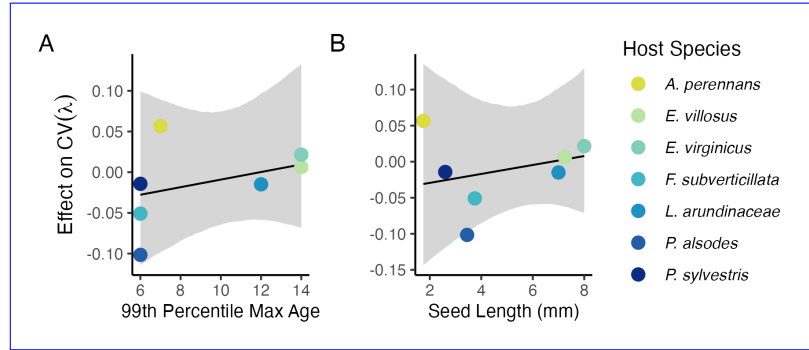
824

825

826

827

828



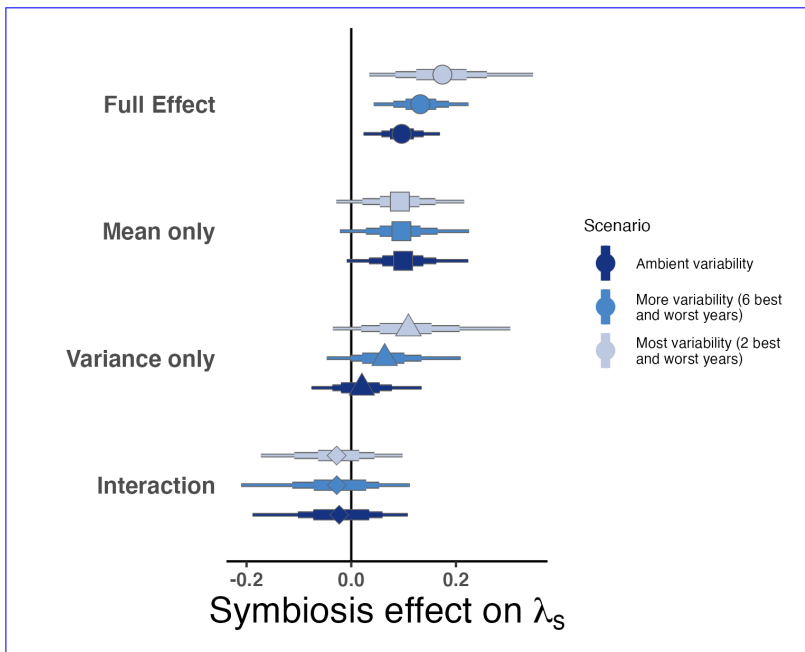


**Fig. 5** Cross-species average endophyte contributions to stochastic growth rates under observed and elevated variance. Endophyte symbiosis contributes to the total effect of mutualism on  $\lambda_S$  through benefits to mean growth rates and through variance buffering as well as the interaction between mean and variance effects. Shapes indicate the posterior mean of each contribution averaged across the seven focal symbiota, along with bars for the 50, 75 and 95% credible intervals. The full effect of the symbiosis (circles) becomes more mutualistic under scenarios of increased variance (represented by color shading). Relative to the ambient scenario sampling transition matrices for all 13 transition years during the study period, simulations increased variance by sampling the most extreme six or two years years, leading to increased contributions from variance buffering effects (triangles) and a constant contribution from mean effects (squares).

829  
830  
831  
832  
833  
834  
835  
836  
837  
838  
839  
840  
841  
842  
843  
844  
845  
846  
847  
848  
849  
850  
851  
852  
853  
854  
855  
856  
857  
858  
859  
860  
861  
862  
863  
864  
865  
866  
867  
868  
869  
870  
871  
872  
873  
874

875 **Supporting Information**

876

877 **Supplemental Methods**

878 **Supplemental Methods**

879

880 **Estimating climate drivers of environmental context-dependence**

881 To connect the variance buffering effects of endophytes with inter-annual variability in climate  
882

883 **Endophyte removal, we built climate-explicit stochastic matrix population**  
884 **models from the vital rate data in addition to the climate-implicit model**  
885 **described in the main text. Identifying the potentially complex relationships**  
886 **between vital rates and environmental drivers remains a key challenge for**  
887 **accurate forecasts of the ecological impacts of environmental stochasticity [?].**  
888 **We first downloaded temperature and precipitation data from a weather**  
889 **station in Bloomington plant propagation, IN, approx. 27 km from our study**  
890 **site, using the rnoaa package [?]. Compared to other weather stations in the**  
891 **area, the measurements from Bloomington contain the most complete climate**  
892 **record across the study period and are correlated with more local**  
893 **measurements field set-up**

894

895 Seeds from naturally symbiotic populations of the seven focal host species were collected  
896 during summer-fall 2006 from Nashville Lilly-Dickey Woods and the nearby Bayles Road  
897 Teaching and Research Preserve (39.220167, IN for years in which local data are available  
898 -86.542683). To generate symbiotic (S+) and symbiont-free (total daily precipitation:  $R^2 =$   
899 -.76; mean daily temperature:  $R^2 = .94$ ). The mean annual temperature across the study  
900 period was  $11.9^{\circ}\text{C}$  ( $\text{SD} = 1.05^{\circ}\text{C}$ ) and the average annual precipitation was 1237.9 mm/year  
901 ( $\text{SD} = 204.89$  mm/year) (Fig. S24). Given the known role of endophytes in promoting host  
902 drought tolerance, we calculated the Standardised Precipitation-Evapotranspiration Index  
903 (SPEI) for 3 and 12 months preceding each annual censuses, reflecting drought during the  
904 growing season and across the year [?]. To calculate SPEI, we used the Thornthwaite equation  
905 to model potential evapotranspiration as implemented in the SPEI R package.

906 S-) plants from the same genetic lineages, seeds from each species were disinfected with a  
907 heat treatment described in Table S1 or left untreated. The heat treatment created symbiont-  
908 free plants by warming seeds to temperatures at which the fungus becomes inviable but the  
909 host seeds can still germinate.

910 We repeated the process of fitting statistical models for each vital rate as described in  
911 **Materials and Methods** with the inclusion of a parameter describing the influence of SPEI.  
912 We fit separate vital rate models incorporating either the growing season or annual drought  
913 index for each vital rate. Both heat-treated and untreated seeds were surface sterilized with  
914 bleach to remove epiphyllous microbes, cold stratified for up to 4 weeks, then germinated  
915 in a growth chamber before transfer to the greenhouse at Indiana University where they  
916 grew for ~ 8 weeks. We confirmed endophyte status by staining thin sections of inner leaf  
917 sheath with aniline blue and examining tissue for fungal hyphae at 200X magnification [?].  
918 We established experimental populations with vegetatively propagated clones of similar sizes  
919 (ranging from one to six tillers).

920 During the fall of 2007 and spring of 2008, we established 10 3x3 m plots for *A. perennans*,  
921 except for the model describing the mean number of seeds per inflorescence. This model was fit  
922 without climate effects because the data came from only a few years. Initial analyses indicated  
923 similar fits for models including only a linear term and those with both linear and quadratic  
924 terms describing the relationship between the climate driver and the vital rate response *E.*  
925 *villosus*, and so we proceeded with models including only the linear term. We expected  
926 that including climate predictors into the models would explain some inter-annual variance  
927 in vital rates *E. virginicus*, shrinking the variance associated with the fitted year random

effects. We assessed model fit with graphic posterior predictive checks—*F. subverticillata*, and *L. arundinaceum* and convergence diagnostics as described for the climate-implicit analysis. Finally, we next built matrix projection models incorporating the climate-dependent vital rate functions to assess the response of symbiotic (S18 plots for *P. alsodes* and *P. sylvestris*). Half of the plots were randomly assigned to be planted with either symbiotic (S+) vs.) or symbiont-free (S-) populations to drought. The model is as described in **Materials and Methods** with the inclusion of parameters describing the slope of the relationship with SPEI. We compared the sensitivity of  $\lambda$  to either annual or seasonal SPEI of S) plants, and initiated with 20 evenly spaced individuals labeled with aluminum tags. In spring 2008, we placed plastic deer net fencing around each plot to limit deer herbivory and disturbance; damaged fences were regularly replaced.

We expected plots to maintain their endophyte status (S+ populations ( $\frac{\Delta\lambda^+}{\Delta SPEI}$ ) with those of or S-populations ( $\frac{\Delta\lambda^-}{\Delta SPEI}$ )(Fig. S25; Table S).

Most species were slightly more responsive to growing season rather than annual drought conditions because these fungal symbionts are almost exclusively vertically transmitted, and plots were spaced a minimum of 5 m apart, limiting seed dispersal or horizontal transmission of the symbiont between plots. We regularly confirmed endophyte treatment throughout the lifetime of the experiment by opportunistically taking subsets of seeds from reproductive individuals and scoring them for their endophyte status with microscopy as above. Overall, these scores reflected 98% faithfulness of recruits to their expected endophyte status across species and plots (Fig. S87; Supplement data). Additionally, we have rarely observed fungal stromata, the fruiting bodies by which *Epichloë* are potentially transmitted horizontally, provided the fly vector is also present [? ]. For *A. perennans*, *F. subverticillata*, *L. arundinaceum*, and *P. alsodes*, we never observed stromata. We observed stromata only infrequently for *E. villosus*, and even more rarely for *E. virginicus* and for most species symbiotic populations were less sensitive to SPEI than symbiont free populations (Fig. S25; Table S3). However *P. sylvestris* (Table S2). For these species, stromata have only been observed irregularly across years on 35, these drought indices did not explain the full extent of inter-annual variability in demographic vital rates. For example, flowering in *A. perennans* had one of the strongest climate signals 4, and 6 plants respectively, making up < 0.3% of all censused plants.

## Detailed vital rate modeling

We fit vital rates models in a Bayesian hierarchical framework. Statistical models for adult survival, seedling survival, adult growth, seedling growth, flowering (yes or no), fertility of flowering plants (number of flowering tillers), production of seed-bearing spikelets (number per inflorescence), the average number of seeds per spikelet, and the recruitment of seedlings from the preceding year's seed production, were constructed as follows:

*Survival* - We modeled survival as a Bernoulli process, where the survival (S) of an individual  $i$  in plot  $p$  and census year  $t$  was predicted by the plot-level endophyte status ( $e$ ), host species ( $h$ ), size in the preceding census, and the plant's origin status ( $o$ ; whether it was initially transplanted or naturally recruited into the plot).

$$S_{i,p,e,h,t} \sim Bernoulli(\hat{S}_{i,p,e,h,t}) \quad (\text{S1a})$$

$$\text{logit}(\hat{S}_{i,p,e,h,t}) = \beta_{0_{h,o}} + \beta_{1_h} * \text{endo}_e \quad (\text{S1b})$$

$$+ \beta_{2_{h,o}} * \text{size}_{i,t-1} + \beta_{3_{h,o}} * \text{size}_{i,t-1}^2 + \tau_{e,h,t} + \rho_p \quad (\text{S1c})$$

$$\tau_{e,h,t} \sim \text{Normal}(0, \sigma_{\tau_{e,h}}^2) \quad (\text{S1d})$$

$$\rho_p \sim \text{Normal}(0, \sigma_\rho^2) \quad (\text{S1e})$$

Here,  $\hat{S}$  is the survival probability,  $\beta_{0_{h,o}}$  is an intercept specific to each host species and recruitment origin,  $\beta_{1_h}$  is the endophyte effect,  $\beta_{2_{h,o}}$  is the effect of plant size specific to each species and recruitment origin,  $\beta_{3_{h,o}}$  is a quadratic plant size effect specific to each species and recruitment origin,  $\tau_{e,h,t}$  is a normally distributed year effect for each species and endophyte

967 status with variance  $\sigma_{\tau_{e,h}}^2$ , and  $\rho_p$  is a normally distributed plot effect with variance  $\sigma_\rho^2$   
968 (82% probability of a positive relationship with SPEI), yet the estimated inter-annual  $p(e)$   
969 indicates that plot identity is uniquely associated with an endophyte status). We assume that  
970 the plot-to-plot variance  $\sigma_{TP}^2$  for symbiont-free plants shrank from 6.7 to 6.1 after including  
971 3-month SPEI as a covariate, suggesting that other factors contribute to  $\sigma_\rho^2$  was shared across  
972 host species, allowing us to “borrow strength” across the multi-species dataset; other model  
973 parameters are unique to host species. We separately modeled the survival of newly recruited  
974 seedlings with a similar model but omitting previous size dependence and origin status.

974 *Growth* - We modeled plant size in census year  $t$  ( $G$ ) with the same linear predictor  
975 for the mean as described for survival. Because we measured size as positive integer-valued  
976 counts of tillers, we modeled it with a zero-truncated Poisson-inverse Gaussian distribution.  
977 This distribution includes a shape parameter  $\lambda_G$  to account for overdispersion in the data.  
978 We additionally modeled the growth of newly recruited seedlings separately with a Poisson-  
979 inverse Gaussian model omitting size structure and the plants’ origin status as with seedling  
980 survival.

980 *Flowering* - We modeled whether or not a plant was flowering during the census ( $P$ ) as a  
981 Bernoulli process, with the same linear predictor for the mean as described above for survival  
982 except that size dependence for reproductive vital rates was determined by the individual’s  
983 size during the same census year as opposed to its size during the previous year.

982 *Fertility* - For a plant that was flowering during the census, its fertility was the number  
983 of reproductive tillers produced ( $F$ ), which we modeled as a function of size in the same  
984 census period with a zero-truncated Poisson-Inverse Gaussian distribution, with the same  
985 linear predictor for the mean as described above.

985 *Spikelets per Inflorescence* - Spikelet production ( $K$ ) was recorded as integer counts on  
986 up to three inflorescences per reproducing plant. We modeled these data with a negative  
987 binomial distribution, with the same linear predictor for the mean as described above.

987 *Seed Production per Spikelet* - For individuals with recorded counts of seed production,  
988 we calculated the number of seeds per spikelet from our counts of seeds and spikelets per  
989 inflorescence, and then modeled seeds per spikelet ( $D$ ) as means of a Gaussian distribution  
990 for each species and endophyte status. Because we had less detailed data across years and  
991 plants for seed production than for other reproductive vital rates, we omitted both plot and  
992 year random effects.

992 *Seedling Recruitment* - We used a binomial distribution to model the recruitment of new  
993 seedlings ( $R$ ) into the plots from seeds produced in the preceding year, assuming no long-  
994 lived seed bank. We included an intercept specific to each host and endophyte status and the  
995 same random effects structure as in other models. We estimated the number of seeds per plot  
996 in the preceding year by multiplying the total number of reproductive tillers per plant by the  
997 mean number of spikelets per inflorescence and mean number of seeds per spikelet ( $D$ ). For  
998 plants with missing fertility or spikelet data, we used the expected number of reproductive  
999 tillers ( $F$ ) or of spikelets per inflorescence from ( $K$ ), drawing from the full posteriors of our  
1000 models. We rounded this value to get the estimated seed production for each individual, and  
1001 finally summed across all reproductive plants in each year and plot to get the total number  
1002 of seeds produced.

#### 1000 **Model assessment**

1001 All parameters were given vague priors [? ]. We ran each vital rate model for 2500 warm-  
1002 up and 2500 MCMC sampling iterations with three chains. We assessed model convergence  
1003 with trace plots of posterior chains and checked for  $\hat{R}$  values less than 1.01, indicating low  
1004 within- and between-chain variation [? ? ]. For those models that showed poor convergence,  
1005 we extended the MCMC sampling to include 5000 warm-up and 5000 sampling iterations,  
1006 which was only necessary for seedling growth. We visualized the interactions between plant  
1007 size, origin status, and endophyte status for both the interannual mean expected value for  
1008 each vital rate (averaging over year and plot variance) (Fig. S2 - S11) and for the expected  
1009 vital rate values specific to each year (averaging over plot variance) (Fig. S12 -S21). We  
1010 graphically checked vital rate model fit with posterior predictive checks comparing simulated  
1011 and observed data (Fig. S30-S68). Initial analyses including only linear effects of size produced  
1012 estimates of endophytes’ effects on vital rate means and inter-annual variability-variances  
1013 that were similar to those from the more flexible quadratic models, but provided worse fit  
1014 to size-structure in the data in some cases. We therefore proceeded with the more flexible

1015

1016

1017

1018

1019

1020

1021

1022

quadratic models. Results from subsequent matrix model analyses were qualitatively similar regardless of this choice. 1013

### Estimating climate drivers of environmental context-dependence 1014

To connect the variance buffering effects of endophytes with inter-annual variability in climate, we built climate-explicit stochastic matrix population models from the vital rate data in addition to the climate-implicit model described in the main text. Identifying the potentially complex relationships between vital rates and environmental drivers remains a key challenge for accurate forecasts of the ecological impacts of environmental stochasticity [? ]. We first downloaded temperature and precipitation data from a weather station in Bloomington, IN, approx. 27 km from our study site, using the rnoaa package [? ]. Compared to other weather stations in the area, the measurements from Bloomington contain the most complete climate record across the study period and are correlated with more local measurements from Nashville, IN for years in which local data are available (total daily precipitation:  $R^2 = .76$ ; mean daily temperature:  $R^2 = .94$ ). The mean annual temperature across the study period was  $11.9 C^\circ$  (SD:  $1.05 C^\circ$ ) and the average annual precipitation was 1237.9 mm/year (SD: 204.89 mm/year) (Fig. S88). Given the known role of endophytes in promoting host drought tolerance, we calculated the Standardised Precipitation-Evapotranspiration Index (SPEI) for 3 and 12 months preceding each annual censuses, reflecting drought during the growing season and across the year [? ]. To calculate SPEI, we used the Thornthwaite equation to model potential evapotranspiration as implemented in the SPEI R package [? ] 1015

We repeated the process of fitting statistical models for each vital rate as described above with the inclusion of a parameter describing the influence of SPEI. We fit separate vital rate models incorporating either the growing season or annual drought index for each vital rate, except for the model describing the mean number of seeds per inflorescence. This model was fit without climate effects because the data came from only a few years. Initial analyses indicated similar fits for models including only a linear term and those with both linear and quadratic terms describing the relationship between the climate driver and the vital rate response, and so we proceeded with models including only the linear term. We expected that including climate predictors into the models would explain some inter-annual variance in vital rates, shrinking the variance associated with the fitted year random effects. We assessed model fit with graphic posterior predictive checks and convergence diagnostics as described for the climate-implicit analysis. Finally, we next built matrix projection models incorporating the climate-dependent vital rate functions to assess the response of symbiotic (S+) vs symbiont-free (S-) populations to drought. The model is as described in **Materials and Methods** with the inclusion of parameters describing the slope of the relationship with SPEI. We compared the sensitivity of  $\lambda$  to either annual or seasonal SPEI of S+ populations ( $\frac{\Delta\lambda^+}{\Delta SPEI}$ ) with those of S- populations ( $\frac{\Delta\lambda^-}{\Delta SPEI}$ ) (Fig. S89; Table S). 1016

Most species were slightly more responsive to growing season rather than annual drought conditions, and for most species symbiotic populations were less sensitive to SPEI than symbiont-free populations (Fig. S89; Table S3). However, these drought indices did not explain the full extent of inter-annual variability in demographic vital rates. For example, flowering in *A. perennans* had one of the strongest climate signals (82% probability of a positive relationship with SPEI), yet the estimated inter-annual variance  $\sigma_{\tau_P}^2$  for symbiont-free plants shrank from 6.7 to 6.1 after including 3-month SPEI as a covariate, suggesting that other factors contribute to inter-annual variability. 1017

### Detailed statistical analysis of life history traits 1018

We fit Bayesian phylogenetic mixed-effects models using the brms package [? ] to test the relationship between each life history trait and the effect of symbiosis on the CV of  $\lambda_t$  (a measure of variance buffering) while controlling for phylogenetic non-independence. We pruned species-level phylogenies of plants [? ] and *Epichloë* fungi [? ] to include the focal species. *Agrostis perennans* was not included in the published tree, and so we used the congener *A. hyemalis*. We defined separate phylogenetic covariance matrices for the pruned tree for host and symbiont species. 1019

1059 We propagated uncertainty in the estimated variance buffering effect  $V$  with a measurement error model:

1061

1062  $V_{MEAN,h} \sim Normal(V_{EST,h}, V_{SD,h})$  (S2a)

1063  $V_{EST,h} \sim Normal(\mu_h, \sigma)$  (S2b)

1064  $\mu = \alpha + \beta * trait + \pi_j$  (S2c)

1065  $\alpha \sim Normal(0, .1)$  (S2d)

1066  $\beta \sim Normal(0, .1)$  (S2e)

1067  $\sigma \sim Half-Normal(.05, .01)$  (S2f)

1068  $\pi_h \sim MVN(0, \sigma_\pi \mathbf{A})$  (S2g)

1069  $\sigma_\pi \sim Half-Normal(0, .1)$  (S2h)

1070

1071 Here,  $V_{EST}$  is the variance buffering effect for host species  $h$ , estimated from the posterior  
1072 mean ( $V_{MEAN}$ ) and standard deviation ( $V_{SD}$ ), propagating uncertainty associated with the  
1073 effect of symbiosis. The model includes an intercept ( $\alpha$ ) and slope ( $\beta$ ) defining the relationship  
1074 between variance buffering effect and the life history trait. The residual standard deviation  
1075 is given by ( $\sigma$ ). We used weakly informative priors to aid model convergence. Each prior  
1076 was centered at zero, except for the residual standard deviation, which we centered at the  
1077 standard deviation of the estimated variance buffering effect, .05. The phylogenetic random  
1078 effect ( $\pi$ ), modeled as a multivariate normal distribution, has a between-species standard  
1079 deviation ( $\sigma_\pi$ ) structured by the phylogenetic covariance matrix  $\mathbf{A}$ . We ran each MCMC  
1080 sampling chain for 8000 warmup iterations and 2000 sampling iterations. We assessed model  
1081 convergence as described above for the vital rate models.

## 1081 **Vital rate mean-variance decomposition**

1082

1083 We performed a mean-variance decomposition to quantify the extent that mean and variance  
1084 effects on stochastic population growth rates arise through different vital rates. Specifically,  
1085 we repeated the calculation of  $\lambda_S$  as described in the main text for symbiotic populations as  
1086 well as symbiont-free populations, as well as for four additional “treatments”. These treat-  
1087 ments differentiate between mortality and growth related vital rates (adult survival, adult  
1088 growth, seedling survival, and seedling growth) and reproductive vital rates (probability of  
1089 flowering, inflorescence production, spikelet production, seed production, and recruitment).  
1090 Each treatment set vital rate mean and interannual variances according to the symbiont-free  
1091 parameter values across vital rates while introducing (1) endophyte effects on the vital rate  
1092 means for survival and growth vital rates only, (2) endophyte effects on the vital rate var-  
1093 iances for survival and growth vital rates only, (3) endophyte effects on the vital rate means  
1094 for reproductive vital rates only, and (4) endophyte effects on the vital rate variances for  
1095 reproductive vital rates only.

1096 The combination of all six  $\lambda_S$  treatments allowed us to quantify to what extent the overall  
1097 effect of symbiosis derives from changes in mean and variance of mortality and growth versus  
1098 in reproductive vital rates. To explore how these contributions could be expected to change  
1099 under increased variability relative to that observed during the study period, we repeated  
1100 this decomposition under the scenarios of increased variance described in the main text,  
1101 sampling transition matrices associated with the set of either six or two most extreme  $\lambda$   
1102 values experienced by symbiont-free populations.

1103 This analysis revealed that both mean and variance buffering effects are driven primarily  
1104 by symbiont effects on survival and growth rather than on reproduction (Fig. S53).

1105

1106

1107

1108

1109

<b>Supplemental Figures S1-S28S1-S89</b>	1105
Supplement figures omitted from track changes	1106
	1107
	1108
	1109
	1110
	1111
	1112
	1113
	1114
	1115
	1116
	1117
	1118
	1119
	1120
	1121
	1122
	1123
	1124
	1125
	1126
	1127
	1128
	1129
	1130
	1131
	1132
	1133
	1134
	1135
	1136
	1137
	1138
	1139
	1140
	1141
	1142
	1143
	1144
	1145
	1146
	1147
	1148
	1149
	1150

1151 **Supplemental Tables S1-S3**

1152 Supplement tables omitted from track changes

1153

1154

1155

1156

1157

1158

1159

1160

1161

1162

1163

1164

1165

1166

1167

1168

1169

1170

1171

1172

1173

1174

1175

1176

1177

1178

1179

1180

1181

1182

1183

1184

1185

1186

1187

1188

1189

1190

1191

1192

1193

1194

1195

1196

## References

- [1] Seneviratne, S. *et al.* *Changes in climate extremes and their impacts on the natural physical environment* (Cambridge University Press, 2012). 1197
- [2] IPCC. Climate change 2021: The physical science basis (2021). URL <https://www.ipcc.ch/report/ar6/wg1/>. 1198
- [3] Bathiany, S., Dakos, V., Scheffer, M. & Lenton, T. M. Climate models predict increasing temperature variability in poor countries. *Science advances* **4**, eaar5809 (2018). 1199
- [4] Swain, D. L., Langenbrunner, B., Neelin, J. D. & Hall, A. Increasing precipitation volatility in twenty-first-century California. *Nature Climate Change* **8**, 427–433 (2018). 1200
- [5] Clark, J. S. Why environmental scientists are becoming bayesians. *Ecology letters* **8**, 2–14 (2005). 1201
- [6] Lewontin, R. C. & Cohen, D. On Population Growth in a Randomly Varying Environment. *Proceedings of the National Academy of Sciences* **62**, 1056–1060 (1969). URL <https://www.pnas.org/content/62/4/1056>. Publisher: National Academy of Sciences Section: Biological Sciences: Zoology. 1202
- [7] Tuljapurkar, S. D. Population dynamics in variable environments. III. Evolutionary dynamics of r-selection. *Theoretical Population Biology* **21**, 141–165 (1982). URL <http://www.sciencedirect.com/science/article/pii/0040580982900107>. 1203
- [8] Cohen, J. E. Comparative statics and stochastic dynamics of age-structured populations. *Theoretical population biology* **16**, 159–171 (1979). 1204
- [9] Tuljapurkar, S. *Population dynamics in variable environments* Vol. 85 (Springer Science & Business Media, 2013). 1205
- [10] Pfister, C. A. Patterns of variance in stage-structured populations: evolutionary predictions and ecological implications. *Proceedings of the National Academy of Sciences* **95**, 213–218 (1998). 1206
- [11] Morris, W. F. *et al.* Longevity can buffer plant and animal populations against changing climatic variability. *Ecology* **89**, 19–25 (2008). 1207
- [12] Compagnoni, A. *et al.* The effect of demographic correlations on the stochastic population dynamics of perennial plants. *Ecological Monographs* **86**, 480–494 (2016). 1208
- [13] Ellis, M. M. & Crone, E. E. The role of transient dynamics in stochastic population growth for nine perennial plants. *Ecology* **94**, 1681–1686 (2013). 1209

- 1243 [14] Murphy, G. I. Pattern in life history and the environment. *The American*  
1244       *Naturalist* **102**, 391–403 (1968).
- 1245  
1246 [15] Davison, R., Stadman, M. & Jongejans, E. Stochastic effects contribute to  
1247       population fitness differences. *Ecological Modelling* **408**, 108760 (2019).
- 1248  
1249 [16] Compagnoni, A. *et al.* Herbaceous perennial plants with short generation time  
1250       have stronger responses to climate anomalies than those with longer generation  
1251       time. *Nature communications* **12**, 1–8 (2021).
- 1252  
1253 [17] Le Coeur, C., Yoccoz, N. G., Salguero-Gómez, R. & Vindenes, Y. Life his-  
1254       tory adaptations to fluctuating environments: Combined effects of demographic  
1255       buffering and lability. *Ecology Letters* **25**, 2107–2119 (2022).
- 1256  
1257 [18] Rodríguez-Caro, R. C. *et al.* The limits of demographic buffering in coping with  
1258       environmental variation. *Oikos* **130**, 1346–1358 (2021).
- 1259  
1260 [19] Tuljapurkar, S. & Orzack, S. H. Population dynamics in variable environments i.  
1261       long-run growth rates and extinction. *Theoretical Population Biology* **18**, 314–342  
1262       (1980).
- 1263  
1264 [20] Fieberg, J. & Ellner, S. P. Stochastic matrix models for conservation and  
1265       management: a comparative review of methods. *Ecology letters* **4**, 244–266 (2001).
- 1266  
1267 [21] Menges, E. S. Applications of population viability analyses in plant conservation.  
1268       *Ecological Bulletins* 73–84 (2000).
- 1269  
1270 [22] Kuparinen, A., Boit, A., Valdovinos, F. S., Lassaux, H. & Martinez, N. D.  
1271       Fishing-induced life-history changes degrade and destabilize harvested ecosys-  
1272       tems. *Scientific reports* **6**, 22245 (2016).
- 1273  
1274 [23] Hilde, C. H. *et al.* The Demographic Buffering Hypothesis: Evidence and Chal-  
1275       lenges. *Trends in Ecology & Evolution* **0** (2020). URL [https://www.cell.com/trends/ecology-evolution/abstract/S0169-5347\(20\)30050-1](https://www.cell.com/trends/ecology-evolution/abstract/S0169-5347(20)30050-1). Publisher: Elsevier.
- 1276  
1277 [24] Rodriguez, R., White Jr, J., Arnold, A. E. & Redman, a. R. a. Fungal endophytes:  
1278       diversity and functional roles. *New phytologist* **182**, 314–330 (2009).
- 1279  
1280 [25] McFall-Ngai, M. *et al.* Animals in a bacterial world, a new imperative for the  
1281       life sciences. *Proceedings of the National Academy of Sciences* **110**, 3229–3236  
1282       (2013).
- 1283  
1284 [26] Funkhouser, L. J. & Bordenstein, S. R. Mom knows best: the universality of  
1285       maternal microbial transmission. *PLoS biology* **11**, e1001631 (2013).
- 1286  
1287 [27] Fine, P. E. Vectors and vertical transmission: an epidemiologic perspective.  
1288       *Annals of the New York Academy of Sciences* **266**, 173–194 (1975).

- [28] Russell, J. A. & Moran, N. A. Costs and benefits of symbiont infection in aphids: variation among symbionts and across temperatures. *Proceedings of the Royal Society B: Biological Sciences* **273**, 603–610 (2006). 1289  
1290  
1291  
1292  
1293  
1294  
1295  
1296  
1297  
1298  
1299  
1300  
1301  
1302  
1303  
1304  
1305  
1306  
1307  
1308  
1309  
1310  
1311  
1312  
1313  
1314  
1315  
1316  
1317  
1318  
1319  
1320  
1321  
1322  
1323  
1324  
1325  
1326  
1327  
1328  
1329  
1330  
1331  
1332  
1333  
1334
- [29] Kivlin, S. N., Emery, S. M. & Rudgers, J. A. Fungal symbionts alter plant responses to global change. *American Journal of Botany* **100**, 1445–1457 (2013).  
[30] Dunbar, H. E., Wilson, A. C. C., Ferguson, N. R. & Moran, N. A. Aphid thermal tolerance is governed by a point mutation in bacterial symbionts. *PLoS biology* **5**, e96 (2007).  
[31] Reyna, R., Cooke, P., Grum, D., Cook, D. & Creamer, R. Detection and localization of the endophyte *undifilum oxytropis* in locoweed tissues. *Botany* **90**, 1229–1236 (2012).  
[32] Saikonen, K., Gundel, P. E. & Helander, M. Chemical ecology mediated by fungal endophytes in grasses. *Journal of chemical ecology* **39**, 962–968 (2013).  
[33] Neyaz, M., Gardner, D. R., Creamer, R. & Cook, D. Localization of the swainsonine-producing chaetothyriales symbiont in the seed and shoot apical meristem in its host *ipomoea carnea*. *Microorganisms* **10**, 545 (2022).  
[34] Chamberlain, S. A., Bronstein, J. L. & Rudgers, J. A. How context dependent are species interactions? *Ecology letters* **17**, 881–890 (2014).  
[35] Catford, J. A., Wilson, J. R., Pyšek, P., Hulme, P. E. & Duncan, R. P. Addressing context dependence in ecology. *Trends in Ecology & Evolution* **37**, 158–170 (2022).  
[36] Jordano, P. Spatial and temporal variation in the avian-frugivore assemblage of *prunus mahaleb*: patterns and consequences. *Oikos* **479**–491 (1994).  
[37] Leuchtmann, A. Systematics, distribution, and host specificity of grass endophytes. *Natural toxins* **1**, 150–162 (1992).  
[38] Cheplick, G. P., Faeth, S. & Faeth, S. H. *Ecology and evolution of the grass-endophyte symbiosis* (OUP USA, 2009).  
[39] Brem, D. & Leuchtmann, A. Epichloë grass endophytes increase herbivore resistance in the woodland grass *brachypodium sylvaticum*. *Oecologia* **126**, 522–530 (2001).  
[40] Decunta, F. A., Pérez, L. I., Malinowski, D. P., Molina-Montenegro, M. A. & Gundel, P. E. A systematic review on the effects of epichloë fungal endophytes on drought tolerance in cool-season grasses. *Frontiers in plant science* **12**, 644731 (2021).

- 1335 [41] Bacon, C. W. & White, J. F. in *Stains, media, and procedures for analyzing*  
1336 *endophytes* 47–56 (CRC Press, 2018).
- 1337
- 1338 [42] Rudgers, J. A. & Swafford, A. L. Benefits of a fungal endophyte in *elymus*  
1339 *virginicus* decline under drought stress. *Basic and Applied Ecology* **10**, 43–51  
1340 (2009).
- 1341
- 1342 [43] Bultman, T. L., White Jr, J. F., Bowdish, T. I., Welch, A. M. & Johnston, J.  
1343 Mutualistic transfer of epichloë spermatia by phorbia flies. *Mycologia* **87**, 182–189  
1344 (1995).
- 1345
- 1346 [44] Stan Development Team. RStan: the R interface to Stan (2022). URL <https://mc-stan.org/>. R package version 2.21.7.
- 1347
- 1348 [45] Elderd, B. D. & Miller, T. E. Quantifying demographic uncertainty: Bayesian  
1349 methods for integral projection models. *Ecological Monographs* **86**, 125–144  
1350 (2016).
- 1351
- 1352 [46] Gabry, J., Simpson, D., Vehtari, A., Betancourt, M. & Gelman, A. Visualization  
1353 in bayesian workflow. *Journal of the Royal Statistical Society Series A: Statistics*  
1354 in Society **182**, 389–402 (2019).
- 1355
- 1356 [47] Brooks, S. P. & Gelman, A. General methods for monitoring convergence of  
1357 iterative simulations. *Journal of computational and graphical statistics* **7**, 434–455  
1358 (1998).
- 1359
- 1360 [48] Gelman, A. & Hill, J. *Data analysis using regression and multilevel/hierarchical*  
1361 *models* (Cambridge university press, 2006).
- 1362
- 1363 [49] Williams, J. L., Miller, T. E. & Ellner, S. P. Avoiding unintentional eviction from  
1364 integral projection models. *Ecology* **93**, 2008–2014 (2012).
- 1365
- 1366 [50] Metcalf, C. J. E. *et al.* Statistical modelling of annual variation for inference  
1367 on stochastic population dynamics using integral projection models. *Methods in*  
1368 *Ecology and Evolution* **6**, 1007–1017 (2015).
- 1369
- 1370 [51] Caswell, H. Matrix population models: Construction, analysis, and interpretation.  
1371 2nd edn sinauer associates. Inc., Sunderland, MA (2001).
- 1372
- 1373 [52] Rees, M. & Ellner, S. P. Integral projection models for populations in temporally  
1374 varying environments. *Ecological Monographs* **79**, 575–594 (2009).
- 1375
- 1376 [53] Jones, O. R. *et al.* Rcompadre and rage—two r packages to facilitate the use of  
1377 the compadre and comadre databases and calculation of life-history traits from  
1378 matrix population models. *Methods in Ecology and Evolution* **13**, 770–781 (2022).
- 1379 [54] .
- 1380

- [55] Bürkner, P.-C. brms: An R package for Bayesian multilevel models using Stan. *Journal of Statistical Software* **80**, 1–28 (2017). 1381  
1382  
1383
- [56] Zanne, A. E. *et al.* Three keys to the radiation of angiosperms into freezing environments. *Nature* **506**, 89–92 (2014). 1384  
1385
- [57] Leuchtmann, A., Bacon, C. W., Schardl, C. L., White Jr, J. F. & Tadych, M. Nomenclatural realignment of neotyphodium species with genus epichloë. *Mycologia* **106**, 202–215 (2014). 1386  
1387  
1388  
1389
- [58] Vicente-Serrano, S. M., Beguería, S. & López-Moreno, J. I. A multiscalar drought index sensitive to global warming: the standardized precipitation evapotranspiration index. *Journal of climate* **23**, 1696–1718 (2010). 1390  
1391  
1392  
1393
- [59] Rudgers, J. A. & Clay, K. An invasive plant–fungal mutualism reduces arthropod diversity. *Ecology Letters* **11**, 831–840 (2008). 1394  
1395  
1396
- [60] Crawford, K. M., Land, J. M. & Rudgers, J. A. Fungal endophytes of native grasses decrease insect herbivore preference and performance. *Oecologia* **164**, 431–444 (2010). 1397  
1398  
1399  
1400
- [61] Rees, M. Evolutionary ecology of seed dormancy and seed size. *Philosophical Transactions of the Royal Society of London. Series B: Biological Sciences* **351**, 1299–1308 (1996). 1401  
1402  
1403
- [62] Moles, A. T. & Westoby, M. Seedling survival and seed size: a synthesis of the literature. *Journal of Ecology* **92**, 372–383 (2004). 1404  
1405  
1406
- [63] Afkhami, M. E. & Rudgers, J. A. Symbiosis lost: imperfect vertical transmission of fungal endophytes in grasses. *The American Naturalist* **172**, 405–416 (2008). 1407  
1408  
1409
- [64] Jeschke, J. M. & Kokko, H. The roles of body size and phylogeny in fast and slow life histories. *Evolutionary Ecology* **23**, 867–878 (2009). 1410  
1411  
1412
- [65] Vandenkoornhuyse, P., Quaiser, A., Duhamel, M., Le Van, A. & Dufresne, A. The importance of the microbiome of the plant holobiont. *New Phytologist* **206**, 1196–1206 (2015). 1413  
1414  
1415  
1416
- [66] Childs, D. Z., Metcalf, C. & Rees, M. Evolutionary bet-hedging in the real world: empirical evidence and challenges revealed by plants. *Proceedings of the Royal Society B: Biological Sciences* **277**, 3055–3064 (2010). 1417  
1418  
1419  
1420
- [67] Brown, A. & Akçay, E. Evolution of transmission mode in conditional mutualisms with spatial variation in symbiont quality. *Evolution* **73**, 128–144 (2019). 1421  
1422
- [68] Bruijning, M., Henry, L. P., Forsberg, S. K., Metcalf, C. J. E. & Ayroles, J. F. Natural selection for imprecise vertical transmission in host–microbiota systems. *Nature ecology & evolution* **6**, 77–87 (2022). 1423  
1424  
1425  
1426

- 1427 [69] Lange, C. *et al.* Impact of intraspecific variation in insect microbiomes on host  
1428 phenotype and evolution. *The ISME journal* **17**, 1798–1807 (2023).
- 1429
- 1430 [70] Yule, K. M., Miller, T. E. & Rudgers, J. A. Costs, benefits, and loss of vertically  
1431 transmitted symbionts affect host population dynamics. *Oikos* **122**, 1512–1520  
1432 (2013).
- 1433
- 1434 [71] Chung, Y. A., Miller, T. E. & Rudgers, J. A. Fungal symbionts maintain a rare  
1435 plant population but demographic advantage drives the dominance of a common  
1436 host. *Journal of Ecology* **103**, 967–977 (2015).
- 1437
- 1438 [72] Tuljapurkar, S. & Haridas, C. Temporal autocorrelation and stochastic population  
1439 growth. *Ecology Letters* **9**, 327–337 (2006).
- 1440
- 1441 [73] Davison, R., Nicole, F., Jacquemyn, H. & Tuljapurkar, S. Contributions of  
1442 covariance: decomposing the components of stochastic population growth in  
1443 cypripedium calceolus. *The American Naturalist* **181**, 410–420 (2013).
- 1444
- 1445 [74] Afkhami, M. E. & Strauss, S. Y. Native fungal endophytes suppress an exotic  
1446 dominant and increase plant diversity over small and large spatial scales. *Ecology*  
1447 **97**, 1159–1169 (2016).
- 1448
- 1449 [75] Smith, E., Vaughan, G., Ketchum, R., McParland, D. & Burt, J. Symbiont  
1450 community stability through severe coral bleaching in a thermally extreme lagoon.  
*Scientific Reports* **7**, 2428 (2017).
- 1451
- 1452 [76] Dallas, J. W. & Warne, R. W. Captivity and animal microbiomes: potential roles  
1453 of microbiota for influencing animal conservation. *Microbial Ecology* 1–19 (2022).
- 1454
- 1455 [77] Wu, L. *et al.* Reduction of microbial diversity in grassland soil is driven by  
1456 long-term climate warming. *Nature Microbiology* **7**, 1054–1062 (2022).
- 1457
- 1458 [78] Ehrlén, J. & Morris, W. F. Predicting changes in the distribution and abundance  
1459 of species under environmental change. *Ecology letters* **18**, 303–314 (2015).
- 1460
- 1461 [79] Chamberlain, S., Hocking, D. & Anderson, B. Package ‘rnoaa’ (2022).
- 1462
- 1463 [80] Beguería, S. & Vicente-Serrano, S. M. Spei: calculation of the standardised  
1464 precipitation-evapotranspiration index. *R package version* **1** (2013).
- 1465
- 1466
- 1467
- 1468
- 1469
- 1470
- 1471
- 1472